Conducting Polymer-based Electrodes for

Electrochemical Supercapacitors

By

Jieming Li, B. Eng.

A Thesis

Submitted to the School of Graduate Studies

In Partial Fulfillment of the Requirements

For the Degree

Master of Applied Science

McMaster University

©Copyright by Jieming Li, April 2017

MASTER OF APPLIED SCIENCE (2017)   McMaster University

(Materials Science and Engineering)   Hamilton, Ontario

TITLE: Conducting   Polymer-based   Electrodes   for Electrochemical Supercapacitors

AUTHOR: Jieming Li, B. Eng. (Beijing University of Technology, China)

SUPERVISOR: Dr. Igor Zhitomirsky

NUMBER OF PAGES: XII, 99

Abstract

Electrochemical Supercapacitors (ESs) have been under investigation for decades as advanced energy storage devices. Selection and fabrication of electrode materials are of vital importance for ESs in terms of energy density, power density, cycling stability, specific capacitance, impedance and other capacitive properties. Among various kinds of materials that can be used for electrode fabrication for ES, Polypyrrole (PPy) is found to be promising due to high specific capacitance, high electric conductivity and low cost of fabrication of this material. The addition of advanced anionic dopant enables higher electric conductivity and the combination of PPy and multiwalled carbon nanotubes (MWCNT) enhances cycling stability of polymer backbone during testing process, which improves capacitive behavior of PPy and the composite materials. Since MWCNT has a relatively high aspect ratio making it difficult to be well dispersed, the selection of effective dispersing agents and dispersion of MWCNT consist an important part of this research.

In this research, PPy and PPy/MWCNT composite materials were synthesized both in chemical and electrochemical ways. The anionic dopants included 4, 5-Dihydroxy-1, 3-benzenedisulfonic acid disodium salt monohydrate (Tiron) and 4-Formylbenzene-1,

3-disulfonic acid disodium salt hydrate (FDS). And also three kinds of multifunctional dopants were used, that can act as dopant for PPy and dispersing agent for MWCNT at the same time, including Eriochrome Cyanine R (ECR), 4-Amino-5-hydroxy-2, 7-naphthalenedisulfonic acid monosodium salt hydrate (AHN) and 3-Hydroxy-4-nitroso-2, 7-naphthalenedisulfonic acid disodium salt (HNN). The molecular size and functional groups of the anionic dopants and dispersants have great influence on the morphology and capacitive properties of PPy and PPy/MWCNT composites. Higher specific capacitance and excellent capacitance retention were achieved by chemical synthesis, which also offers advantages for large scale production.

The results showed that with dopants possessing larger molecular size and multiple charged groups, smaller particle size of PPy and improved capacitive properties could be obtained. The PPy/MWCNT mass ratio of 7 to 3 and Py monomer to dopant molecule molar ratio of 3 to 1 were found to be optimal. The use of Ni foam current collector enabled high mass loading of active materials, which facilitates the fabrication of advanced electrodes for supercapacitors.

Acknowledgements

I hereby express my deepest gratitude to my supervisor Professor Igor Zhitomirsky for his intellectual guidance and continuous encouragement and support. I appreciated the environment of enthusiasm towards nature and science Professor has created and I wish greater success for Professor Igor Zhitomirsky in the future.

I am grateful to my committee members for their time, patience and criticism as well. I also want to thank Kaiyuan Shi, Dan Luo, Mustafa Ata, Cameron Wallar, Yangshuai Liu and Patrick Wojtal for their kindness of helping me all along my two years of Master's research life. To all my group colleagues, Tianshi Zhang, Xinya Zhao, Haoyu Fan, Ryan Poon and Amanda Clifford, many thanks to your help and support. It is my honor to work with you.

I want to express gratitude to Canadian Centre for Electron Microscopy and other faculty and staff in MSE department and in McMaster University. I would not have accomplished my thesis research without you.

Finally, great thanks to my parents, my boyfriend Pengfan Wang for supporting me through my hardest time studying abroad on my own and all of my friends I made in Canada for the help in life and company so that I do not feel lonely any more.

Table of Contents

List of Figures

List of Tables

1. Introduction

Developing new energy storage devices has attracted very much attention in recent years due to climate change and limited resource of fossil fuels. With increasing demand for advanced portable electronic devices, hybrid vehicles and machines for special operations, people started looking for new power sources a long time ago and supercapacitors have been brought into sight. Electrochemical Supercapacitor (EC), also called Supercapacitor or Ultracapacitor [1], has capacitive behavior through either electric double layer or fast and reversible redox reactions. Supercapacitors can store much more energy compared to conventional capacitors because of their high surface area and atomic size distance between the electrode surface and electrolyte surface. The fast and reversible charging-discharging kinetics of supercapacitors allow relatively high power density compared to batteries. Electrochemical properties depend strongly on electrode materials and electrolytes. Various kinds of materials can be used for the electrodes, including metal oxides, conducting polymers (CPs) and composites.

CPs based materials for supercapacitors have gained very much attention due to their high specific capacitance (SC), high electric conductivity in doped state, low cost of fabrication and easy polymerization [2]. Among various CPs, Polypyrrole (PPy) is a

promising material, which has been used in this investigation. PPy synthesis can be accomplished by electrochemical or chemical polymerization methods. Electrochemical deposition of PPy has been under investigation for a long time, but relatively low mass loading of active materials (<1 mg cm^{-2}) and low deposition efficiency on non-noble substrates have restricted its practical applications. On the contrary, chemical synthesis of PPy powders is more effective and with pasting powders onto current collector nickel foam, mass loading can be controlled within the range of 10 mg cm^{-2} to 40 mg cm^{-2} [3]. Also, highly porous nickel foam current collector can support porous structure of PPy powders, which is beneficial for access of electrolyte and electrochemical properties of PPy electrode.

The conductivity of PPy can be increased by doping with counter ions and PPy can only be P-doped. Anionic dopants have great influence on the conductive properties of PPy electrodes. In my research, I used Tiron, FDS, ECR, AHN and HNN as dopants and ECR, AHN and HNN are multifunctional dopant which can act as a dopant for PPy and dispersing agent for MWCNT. Based on previous group investigation, we are looking for dopants with specific structures and functional groups. And it is an original research conducted to investigate the influence of dopants on PPy morphology and capacitive behavior.

The biggest drawback of pure PPy material is its poor mechanical stability, which leads to degradation of bulky materials due to shrinkage and swelling. It is the cause of poor retention of the electrode and short cycle life. To deal with the problem, synthesis of composites containing PPy and MWCNT improves the cycling stability of the electrode material. However, because of the high surface area of MWCNT, it is possible for MWCNTs to agglomerate and very difficult to get uniform dispersion of MWCNT. Another important part of my work is to optimize the selection of dispersants, which is one of the main factors affecting morphology and capacitive properties of PPy/MWCNT composites.

2. Literature Review

2.1 History of Supercapacitors

The concept of electrical energy storage in electric double layer formed at the interface of electrode and electrolyte was brought up in the late 1800s. The first device using double layer charge storage mechanism was designed in1957 by H.I. Becker from General Electric (U.S. Patent 2,800,616), but the device never got commercialized. Later, a chemist from the Standard Oil Company of Ohio (SOHIO), Rober A. Rightmire invented the device in the format that is commonly used now. His patent (U.S. 3,288,641) was

filed in 1962, followed by another researcher from SOHIO, Donald L. Boos who founded

the basis for subsequent patents and papers of aspects of electrochemical supercapacitor

technology. Later in 1975, a new mechanism of energy storage was developed by

Conway, in which energy was generated and released from redox reactions taking place

on electrode materials. It involved adsorption and desorption of hydrogen and metal ions,

such as Pb, Bi and Cu on noble current collectors. Three years later, the first production

of supercapacitor was introduced to commercialization and the license was held by

SOHIO. After commercialization, electrochemical supercapacitors acted as a back-up

power source for volatile and complementary metal-oxide-semiconductor (CMOS)

computer memories. Many other applications have been developed over the past 30 years,

such as portable electronic devices and high-efficiency energy storage device for electric

vehicles and hybrid electric vehicles. Many companies were involved in emerging

development and applications of supercapacitors, such as SOHIO, NEC, ECOND,

PANASONIC, ELIT, ELNA, MAXWELL, ESMA, CAP-XX, NIPPON CHEMI-CON

and NESSCAP [4].

2.2 Energy Storage Devices

2.2.1 Comparison between Devices

Fossil fuels have played an important role in the development of industry and society, but

the environmental pollutions caused by greenhouse gas emission are severe enough as a reminding of searching for new energy source and energy storage devices. There are mainly four types of energy storage systems and devices, including conventional capacitors, batteries, fuel cells and electrochemical supercapacitors [5]. Conventional capacitors store electric energy by inserting a dielectric material between two conducting plates, which are usually made of metals. The dielectric materials are polarized when connected to an external power source and being charged, in which way capacitors can store more charges. The amount of energy can be stored is related to charges accumulated on metal plates. The maximum potential applied to conventional capacitors is limited by the dielectric material breakdown field [6]. An ideal electrostatic capacitor is characterized by a constant capacitance C, which is the capability of charge storage and can be calculated by the amount of accumulated charge (Q) and the applied potential (V).

$$C = \frac{Q}{V} \qquad \text{2-1}$$

Capacitance is an important parameter of capacitor devices and it is determined by properties of dielectric materials inserted between the conducting plates. When two parallel plates are separated by vacuum in the region between the plates, the capacitance can be expressed in the following way [7],

$$C = \varepsilon \frac{A}{d} \qquad \text{2-2}$$

where A is the total area of one conducting plate, d is the distance of two conducting plates and ε is the permittivity of a vacuum with a constant value of 8.85×10^{-12} F m^{-1} that represents the capability of energy storing strength of a vacuum. The capacitance of the double-layer supercapacitors can be estimated in a similar way. Energy stored in capacitors can be characterized by the following equation,

$$W = \int_0^Q V dq = \int_0^Q \frac{q}{C} dq = \frac{1}{2}\frac{Q^2}{C} = \frac{1}{2}CV^2 \qquad \text{2-3}$$

where C is the capacitance and V is the potential applied to it. And maximum power of capacitors is determined by the equation shown here,

$$P = \frac{W}{t} = \frac{1}{2}VI = \frac{1}{4}\frac{V^2}{R} \qquad \text{2-4}$$

where R is the equivalent series resistance. The parameters are always mass or volume normalized.

Unlike capacitors, batteries generate faradaic current through redox reactions of the electrode or substrate materials and electrolyte, which comes with phase change and some part of the reaction is irreversible [8]. In fuel cells, chemical energy is converted into electric energy through redox reactions of fuel with catalyst (Pt), which makes it more like an energy generator than an energy storage device [9]. Figure 2-1 shows the

Ragone plot that is named after D.V. Ragone [10] and it is the comparison between different energy storage devices in terms of energy density and power density. Energy density is how much energy can be stored in the device, while power density is how fast energy can be delivered. Fig. 2-1 presents mass normalized parameters, from which we can clearly conclude that conventional capacitors have relatively high power density but very low energy density. In capacitors, the energy is stored by electrostatic adsorption of electrons onto the conducting plates. The capacitance is limited by the dielectric material inside, but the energy can be released in a very fast way. Batteries and fuel cells obviously can store and generate much more energy but they have fairly low power density because of the redox reactions and ions diffusion they have to go through when delivering begins. Electrochemical supercapacitors, to some degree, bridge the gap between conventional capacitors and batteries with higher powder and energy densities at the level of $\sim 10^3$-10^4 W kg^{-1} and $\sim 10^0$-10^1 Wh kg^{-1}, respectively. Their advantages make them applicable for a wide scope of applications, including high power and energy densities, fast charging-discharging kinetics (1-30s), high efficiency (> 95%), long cycle life (> 10^6 cycles), easy processability and ecological friendliness and low cost [1, 6, 11].
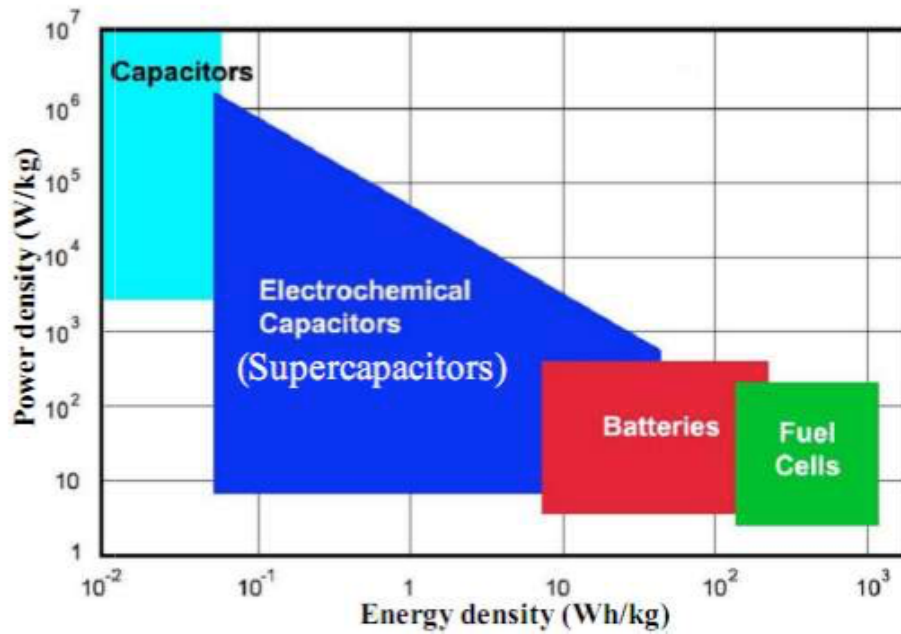
Fig 2-1 Ragone Plot (Power density of several kinds of energy storage devices versus Energy density) [12]
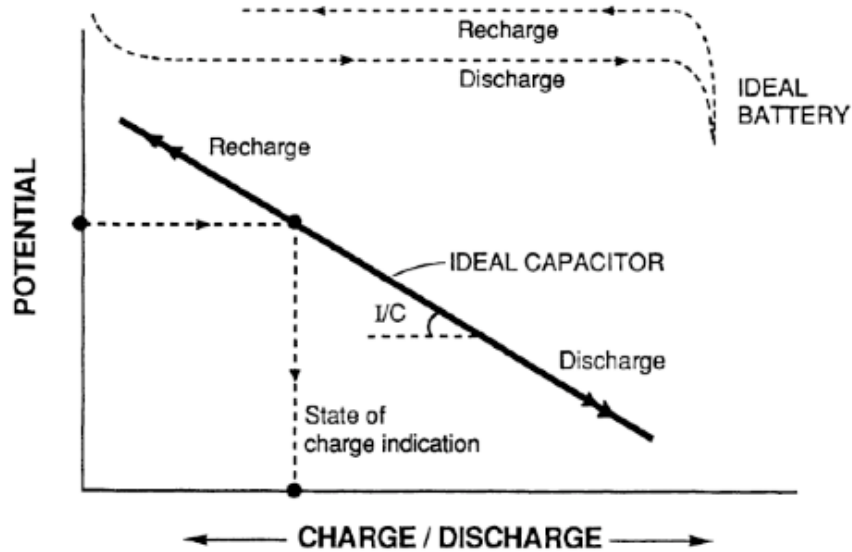
Fig 2-2 Charge-discharge curves of ideal battery and ideal capacitor [6]

For ideal batteries, when charging and discharging process begin, the potential remains constant throughout the whole process. On the contrary, in an electrochemical supercapacitor, accumulated charges have a linear relationship with the potential across electrodes [6].

2.2.2 Applications of Electrochemical Supercapacitors

Electrochemical supercapacitors can find applications in many areas, including portable electronic devices, huge industrial machines and hybrid vehicles, etc [6, 13].

Due to the fast charging-discharging kinetics of electrochemical supercapacitors, it is a promising and ideal device for applications involving high power output and uninterruptible power supply [14], such as flash light of smart phone, turning on of smart phone and power source for desktop or laptops. Supercapacitors can also be used in hybrid vehicles and automobiles [15]. Supercapacitors can generate energy from braking system and release energy for acceleration of vehicles or climbing uphill. In applications in huge industrial machines like mining shovel [16], supercapacitors capture and collect energy from swing deceleration and deliver burst energy to assist lifting operations, which is reportedly said to be able to save 25% of fuels demanded. Since supercapacitors can act as extra power source [17], they can provide back-up energy if there is a power shutdown of main power source in houses, aircraft doors and data centers and thus enhance safety of daily human life and information security.

Fig 2-3 Applications of supercapacitors in portable electronics, hybrid vehicles, huge industrial machines, houses, aircraft doors and data centers.

2.3 Mechanisms of Energy Storage in Supercapacitors

ES has been under development for over 30 years. At first, supercapacitors were limited to double layer mechanism, which leads to low energy density and fairly high cost [6]. The situation was changed historically by Conway in 1975 who brought up another mechanism of energy storage system, energy generated from Faradaic charge exchange. ES can be divided into three categories based on energy storage mechanism: (1) Electrochemical Double Layer Capacitors (EDLCs), (2) Pseudocapacitors and (3) hybrid capacitors.

2.3.1 Electrochemical Double Layer Capacitors

EDLC is the kind of supercapacitor that store energy through non-Faradaic process. It involves adsorption/desorption of charges on the electric double layer that refers to two parallel layers of opposite charges accumulated at the interface of electrode and electrolyte. At macroscopic level, how EDLCs store much more energy can be explained by the equation $C=\varepsilon_0 A/d$. EDLCs have very large surface area A because of the porous structure of bulk electrode materials and a relatively small gap d between the separated charges that is of atomic level. The specific surface area has been recorded to reach 1000-2000 m^2 cm^{-3} [18], which is why capacitances of conventional capacitors are delivered in mF and μF quantities but with supercapacitors delivering is in the unit of hundreds or even thousands of Farads [19].
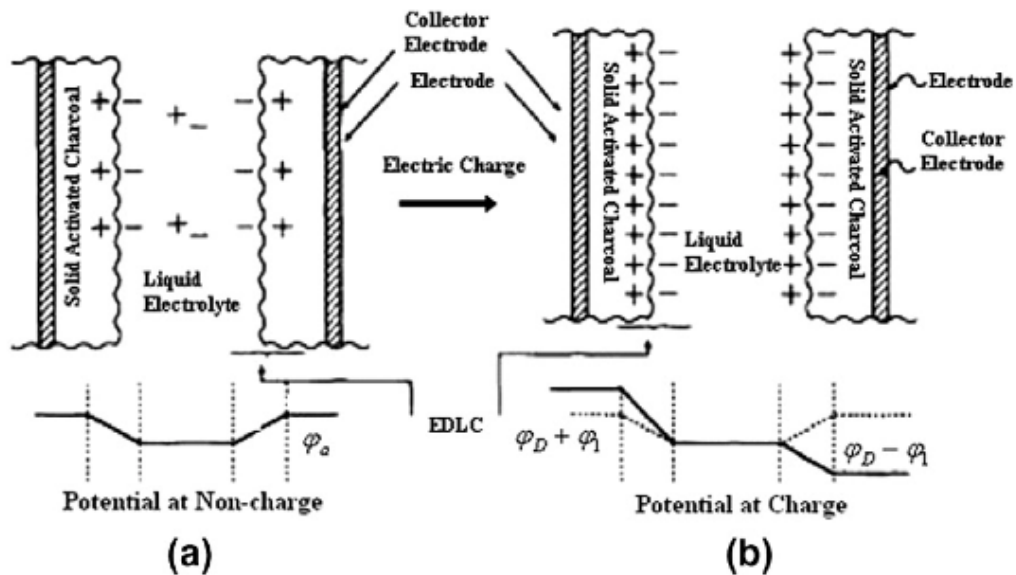
Fig 2-4 Charge storage mechanism of EDLCs [20]

During the charging process, positive electrode is stacked with positive charges and in the electrolyte anions are attracted to positive electrode while cations move to negative electrode to form two double layer capacitors connected in series. In each EDLS cell, two electrodes can be considered to be two individual capacitors and the total capacitance of the cell can be described in the following equation,

$$C_{cell} = (\frac{1}{C_1} + \frac{1}{C_2})^{-1}$$ 2-5

where C_1 and C_2 are the capacitances of two double layer capacitors.
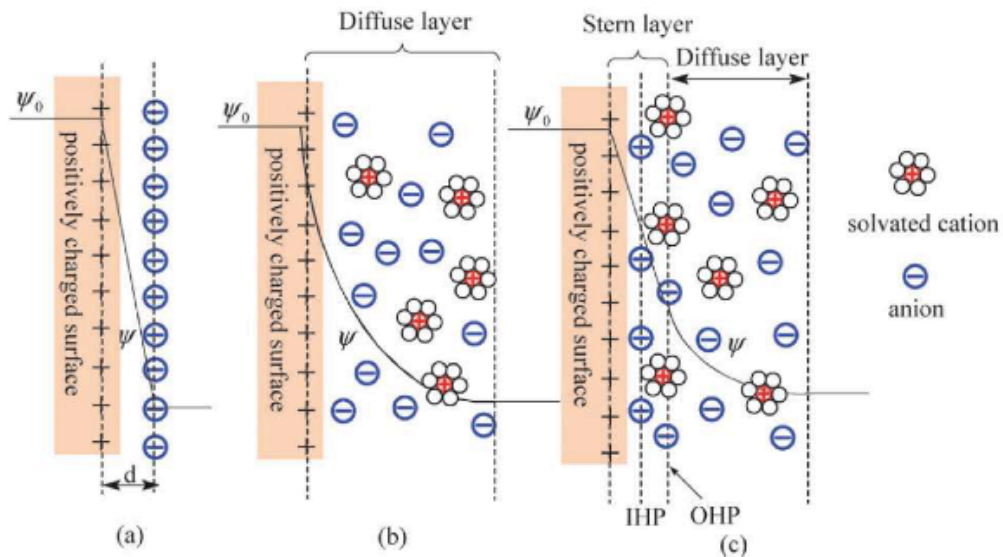
Fig 2-5 Models of double layer: (a) Helmholtz model, (b) Gouy-Chapman model and (c) Stern model with IHP indicating inner Helmholtz plane and OHP indicating outer Helmholtz plane. ψ_0 and ψ are potentials at the electrode surface and the electrode/electrolyte interface, respectively [6].

The concept of a double-layer was originally described by von Helmholtz in the 19th

century in his investigation of the distribution of opposite charges at the interface of

colloidal particles and the model is shown in Fig 2-5 .The model was later adapted to the

electrode interface. In the Helmholtz model (Figure 2-5 (a)), the double-layer of the

electrode interface consists of two layers of opposite charges formed at the

electrode/electrolyte interface, which are separated by an atomic distance. After

Helmholtz's model was proposed, it became realized that ions on the solution side of the

double-layer could not remain static in a compact array but could be subject to the effects

of thermal fluctuation according to the Boltzmann principle. This simple Helmholtz

double-layer model was further modified by Gouy and Chapman. The Gouy–Chapman

model (Figure 2-5 (b)) then proposed that the continuous distribution of ions in the

electrolyte solution could be described by a diffuse layer with a distance of d due to the

thermal fluctuation. In this model, the ions were assumed to be point charges. However,

the capacitance of two separated arrays of charges increases inversely with their

separation distance, which leads to a very large capacitance value in the case of point

charge ions close to the electrode surface. Later, Stern combined the Helmholtz model

and the Gouy–Chapman model to explicitly demonstrate two layers of ion distribution,

the compact layer and the diffuse layer. The compact layer consists of inner Helmholtz

plane (IHP) and outer Helmholtz plane (OHP). The IHP refers to the distance of closest

approach of specifically adsorbed ions and OHP is that of the non-specifically adsorbed

ions. The OHP is also the plane where the diffuse layer begins. In the 1950s, Grahame [21] made a distinction between IHP and OHP in the interfaces which corresponds to different distances of closest approach. This difference is mainly caused by the fact that most cations are smaller than common anions and retain solvation shells due to strong ion-solvent dipole interaction. It has been demonstrated that the capacitance of the double-layer is also dependent on the surface properties of electrode, the ions of electrolyte and the solvent [22].

2.3.2 Pseudocapacitors

Another type of electrochemical supercapacitors is pseudocapacitor and when a potential is applied to a pseudocapacitor, fast and reversible redox reactions take place on the electrode material, not only on the surface, but inside the bulk material. Materials that will undergo redox reactions include conducting polymers (CP) and metal oxides, such as RuO_2, MnO_2 and Co_2O_3 [2]. There are basically three types of faradaic process going on with the electrode material, which are reversible adsorption/desorption, redox reactions of transition metal oxides and reversible electrochemical doping/dedoping of counter ions in CPs [6, 19, 23]. The following table is a comparison between pseudocapacitor and electrochemical double layer capacitors. Obviously pseudocapacitors have higher energy density because their interior electrode materials are involved in redox reactions rather than that just the surface atoms are involved in double layer capacitors and as reported by

Conway *et al.* [6] the capacitance of a pseudocapacitance can be 10–100 times higher than the electrostatic capacitance of an EDLS. However, on the other hand, EDLCs have higher power density because electric energy is stored through electrostatic attractions and it takes much less time to be released. When it comes to reversibility and cycle life, there are partly irreversible reactions take place in conducting polymers and other pseudocapacitor electrode materials, which leads to degradation of cyclic stability of electrodes. It has been reported that the Faradaic processes in pseudocapacitors can benefit from extending voltage window of the device, which is of vital importance because energy power densities are linear to V square [6].

Table 2-1 Comparison between EDLCs and Pseudocapacitors [24]

Double-layer capacitance

1. Non-faradaic
2. $20–50~\mu F~cm^{-2}$
3. C fairly constant with potential, except through the p.z.c.
4. Highly reversible charging/discharging
5. Has restricted voltage range (contrast non-electrochemical electrostatic capacitor)
6. Exhibits mirror-image voltammograms

Pseudocapacitance

1. Involves faradaic process(es)
2. $2000~\mu F~cm^{-2}$ for single-state process; $200–500~\mu F~cm^{-2}$ for multi-state, overlapping processes
3. C fairly constant with potential for RuO_2; for single-state process, exhibits marked maximum
4. Can exhibit several maxima for overlapping, multi-state processes, as for H at Pt
5. Quite reversible but has intrinsic electrode-kinetic rate limitation determined by R_f
6. Has restricted voltage range
7. Exhibits mirror-image voltammograms

B.E. Conway demonstrated that pseudocapacitive behavior can be achieve by several faradic mechanisms: (1) underpotential deposition, (2) redox pseudocapacitance and (3) intercalation pseudocapacitance [25], which is illustrated in Fig 2-6.
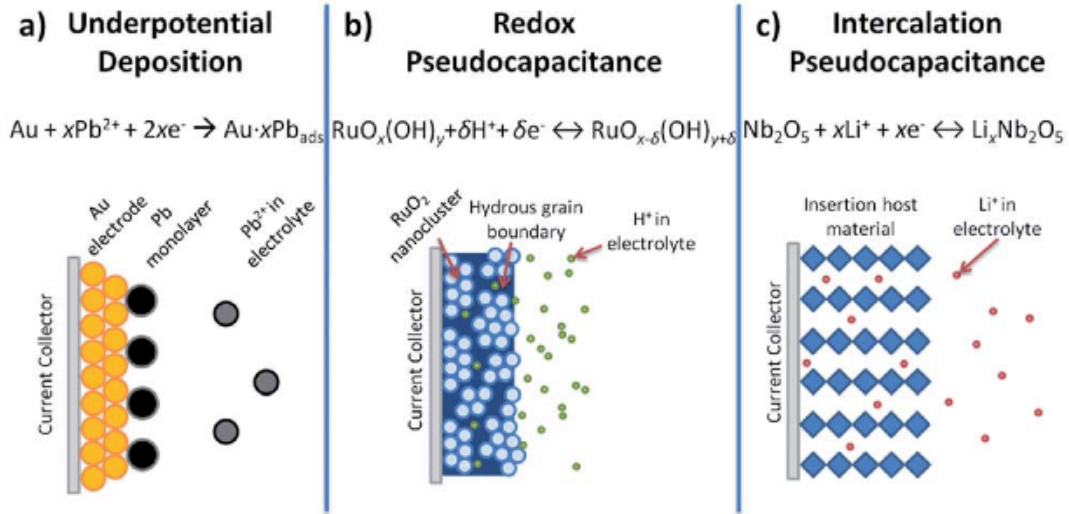
Fig 2-6 Different pseudocapacitive mechanisms: (a) underpotential deposition, (b) redox pseudocapacitance and (c) intercalation pseudocapacitance [6]

Underpotential deposition takes place when metal ions are adsorbed and form a monolayer at a different metal's surfaces well above their redox potential. Redox pseudocapacitance occurs when ions are electrochemically adsorbed onto the surface or near surface of a material accompanied with a faradaic charge transfer process. Intercalation pseudocapacitance happens when ions penetrate into the pores and tunnels of a redox-active material, which is accompanied with a faradaic charge transfer process but without any phase transformation. These three mechanisms occur due to different physical processes and with different types of materials.

2.3.3 Hybrid Supercapacitors

Traditional ES device consists of two electrodes made from same materials, which is a symmetrical ES [26, 27]. The open circuit voltage of a symmetrical ES is the same as the voltage window of a single electrode. Since voltage window plays an important role in electrochemical properties of supercapacitor devices, hybrid supercapacitors were developed and designed with one electrode made of materials storing energy through non-Faradaic mechanism and the other electrode consist of pseudocapacitor type of material.

2.4 Electrode Materials for Electrochemical Supercapacitors

Since there are mainly two mechanisms of electrochemical supercapacitor (electrochemical double layer and redox-based capacitance) and ES are divided into three categories (EDLCs, Pseudocapacitors and Hybrid capacitors), for each mechanism or individual category, certain materials can fulfill the requirements [28, 29].

2.4.1 Carbon-based Materials

EDLCs can achieve extremely high capacitance due to high specific surface area and small gap between arrays of charges, which indicates that surface area and electric conductivity of the electrode materials are of vital importance for capacitive behavior of the devices [30]. Also, cyclic stability, temperature adaptability, cost for processing, ions

in electrolyte and etc. are other factors that should be taken into consideration for selection of the electrode materials.

Carbon materials are considered promising electrode materials for practical application due to their micropore structures, high specific surface area, excellent electric conductivity, high chemical and physical stabilities and lower cost [31]. Carbon materials are a typical example of double layer charge storage theory, which makes the capacitive behavior more dependent on the accessibility of electrolyte ions towards electrode surface [24]. Important factors for selecting carbon-based electrode materials include pore size distribution, micropore structure, and specific surface area. Among them, specific surface area and pore size distribution are two key factors that have a strong influence on the materials performances [1]. Many efforts have been invested into developing methods for increasing specific surface area, such as heat treatment, alkaline modification, plasma surface modification and so on. Carbon materials that are commonly used include activated carbon, carbon nanotubes (CNTs), carbon aerogels, template porous carbons and carbon nanofibers [2, 23].
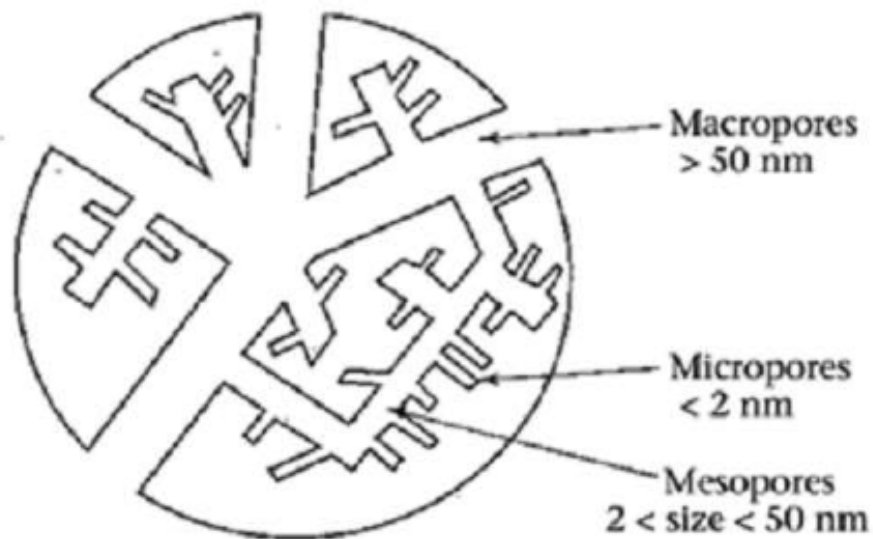
Fig 2-7 Schematic network of pore size distribution for activated carbon [3]

P. Simon and A. Burke demonstrated pore size distribution in activated carbon grain, which is shown in Fig 2-7. The theory can be applied to various kinds of carbon materials for electrode of EDLCs. The pores can be classified into three categories based on size: micropores (< 2 nm), mesopores (2-50 nm) and macropores (> 50 nm) [32]. Among them, micropores are said to contribute the most to capacitive properties of electrodes, but only up to 20 nm in the depth of surface can be reached, limited by diffusion related conditions [32]. However, if the pores are so small that they are not accessible for electrolyte ions, it contributes no more and therefore, pore size should be optimized for electrolyte ions and usually smaller particle size of electrode material results in larger pore surface areas.

2.4.2 Pseudo-capacitive Materials

Capacitance generated from Faradaic charge transfer also exists in carbon based materials, but the contribution is so little that we can even overlook. Metal oxides and conducting polymers, however, are predominantly manipulated by redox reactions [6].

2.4.2.1 Metal Oxides

Several kinds of metal oxides have been under investigation for applications in supercapacitors, such as ruthenium oxides, manganese oxides, cobalt oxides, nickel oxides and vanadium oxides [2]. Certain requirements should be met if a metal oxide is chosen as the electrode material for electrochemical supercapacitors, including that it should be electrically conductive, and the metal must have multiple valence states so that redox reactions can take place and protons can easily intercalate into and detercalate from the lattice during charging and discharging processes. Among the metal oxides, RuO_x has attracted the most intense attention due to its wide potential range reaching 1.2 V that contributes very much to energy and power densities of the device, highly reversible redox reactions that elongate cycle life, multiple valence states, high thermal stability and other properties [2]. It was reported that the capacitive performances arise from double layer charge storage contribute 10% of the total specific capacitance. For pseudocapacitive behavior, with different environments, the capacitive performance of ruthenium oxides varies due to different sensitivities to environment. In an acidic

environment, the reversible redox reaction is shown by the following equation, with

protons adsorbed on the surface of RuO$_2$ and Ru changes from Ru (IV) to Ru (II).

$$RuO_2 + xH^+ + xe^- \leftrightarrow RuO_{2-x}(OH)_x \qquad\qquad 2\text{-}6$$

On the contrary, when RuO$_2$ is in alkaline environment, the changes in valence state are

complicated. RuO$_2$ can end up in multiple forms such as RuO$_4^{2-}$, RuO$_4^-$ and RuO$_4$ [22].

However, when it comes to cost, RuO$_2$ is not the ideal candidate for commercialized

supercapacitors because of its high cost [33, 34]. Recently researchers are making efforts

to select substitutional metal oxides that are cheaper but perform as well as Ru oxides.

However, it is limited by the usage of acidic electrolyte. Good capacitive performances of

metal oxides depend greatly on adsorption of protons, but with strong acid, metal oxides

have massive possibilities of dissolution [35, 36]. Neutral electrolytes are taken into

consideration like Na$_2$SO$_4$ and KCl for manganese, cobalt, iron and nickel oxides.

Among these metal oxides, MnO$_2$ has attracted very much attention with a theoretical

capacitance reaching 1380 F g^{-1} [36, 37]. The charge-discharge reaction is shown in

Equation 2-7, which contributes to the capacitive behavior of manganese dioxide with the

exchange of protons or cations and transitions in valence states of manganese.

$$MnO_2 + xC^+ + yH^+ + (x+y)e^- \rightarrow MnOOC_xH_y \qquad\qquad 2\text{-}7$$
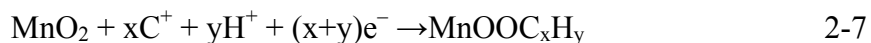
2.4.2.2 Conducting Polymers

The first reported conductivity of conducting polymer (CPs) was in 1963 by Weiss and other coworkers in Australia [38, 39] and later conducting polymers were utilized in supercapacitors for the first time in the mid 1990s. CPs are conductive due to the conjugate bond system along the polymer chains, which makes electrons no more fixed and easier to move around. P-doped CPs are formed through oxidation of monomers. The polymer may have lower oxidation potential so that two oxidation reactions take place at the same time, the oxidation of monomers and the oxidation of the polymer chains. This is the reason that we dope CPs with counter ions or dopants to compensate charges, keep products neutral and increase conductivity of CPs. Depending on the redox type reactions and polarity of dopant molecules, CPs are classified into two types: n-doped and p-doped [6]. N-doped CPs are reduced during charging and doped with cationic dopants while oxidation takes place on p-doped CPs when being charged. It has been reported that p-doped CPs are more stable than N-doped CPs and also have wider scope of applications in electrochemical supercapacitors [40].
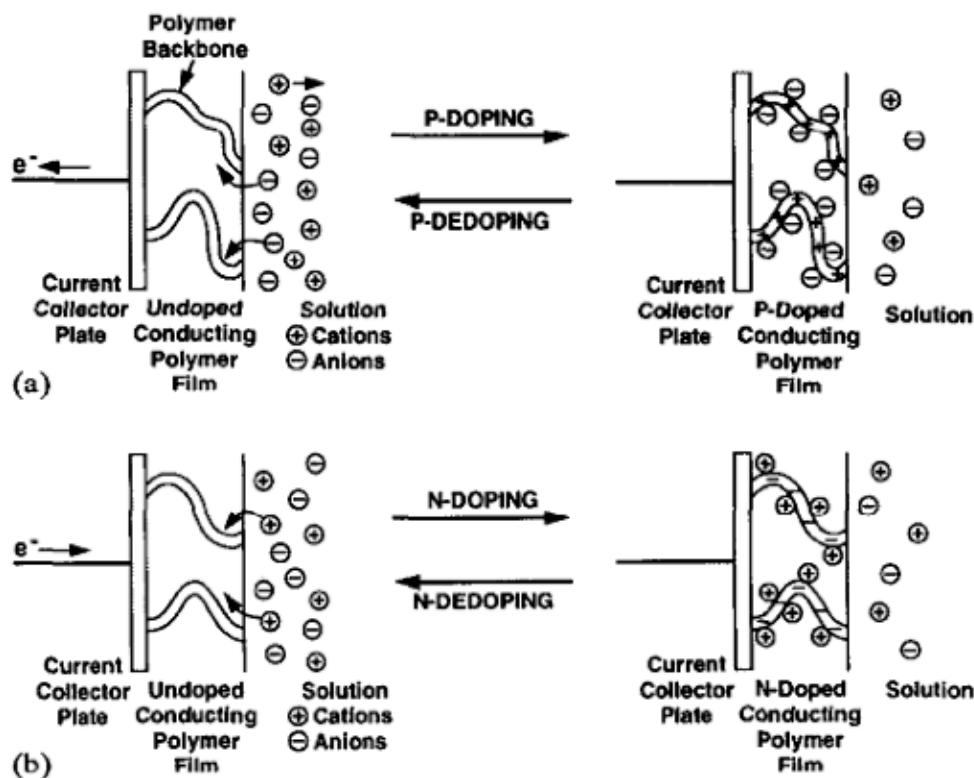
Fig 2-8 Sketch of (a) p-doping and (b) n-doping of CPs [6]

Doping level varies for different kinds of CPs because doping is related to how closely

the positive or negative charges are spaced along the polymer backbone and for p-doped

type of CPs, the doping level is approximately 0.3-0.5 dopant molecule per monomer

[19]. One of the advantages of CPs is lower cost for fabrication compared with some

expensive metal oxides such as RuO_x. Devices using CPs as electrode materials may not

perform as well as metal oxides, however, when compared to carbon based materials,

they present much better capacitive properties. It is reported that Polyaniline (PAni) can

reach a charge density of 140 mAh g^{-1} [19], but carbon devices only generate less than 15

mAh g^{-1} [19]. And as for energy and power densities, devices with CPs like PAni can exhibit a high energy of 10 Wh kg^{-1} but a lower power of 2 kW kg^{-1}, while carbon devices can only store less than half the energy of CPs devices of 3-5 Wh kg^{-1} but show higher power of 3-4 kW kg^{-1} [19, 40]. This is because carbon devices are based on double layer mechanism, which is purely electrostatic attraction between opposite charges and only occurs on the surface of electrodes so that the charge release is fast when discharging. On the contrary, capacitance of CPs is based on pseudocapacitive mechanism and it takes longer time to accomplish redox reactions during charging-discharging process, but with interior bulk materials on the electrode involved in charge storage, the device has a higher energy density.

Table 2-2 Properties of four kinds of CPs

Polymer	Doping level	Potential range (V)	Theoretical SC (F g-1)	Conductivity (S cm-1)	Doping type
PPy	0.33	0.8	620	10-50	P-doping
PAni	0.5	0.7	750	0.1-5	P-doping
PTh	0.33	0.8	485	300-400	n, P-doping
PEDOT	0.33	1.2	210	300-500	n, P-doping

2.4.2.3 Composite Materials

Since metal oxides and conducting polymers share pseudocapacitive energy storage mechanism, they store much more charges than EDLCs. But carbon materials are more stable and have excellent electric conductivity and longer cycle life due to the reversibility of electrostatic adsorption/desorption of ions. If combined together, metal oxides and CPs will show better retention due to enhanced mechanical stability and good capacitive behavior because of improved conductivity. With the usage of carbon materials as a scaffold, electrode material can be more porous, which contributes to large capacitance due to higher specific surface area. Composite electrodes are made of one type of material incorporated into another material, typically a layer of pseudocapacitive material coating on carbon materials. Usually pseudocapacitive materials have higher energy density sacrificing mechanical stability, cycle life, electric conductivity and power density. The strategies of making composite materials with enhanced energy and power densities are shown in Fig 2-9. Significant attention has been generated on pseudocapacitive material/MWCNT composites as electrode materials. The addition of CNTs is beneficial due to their high surface area and excellent electric conductivity. The conducting polymer-CNTs can enhance polymer cyclic stability and elongate cycle life, which can be backed up with the fact that after adding CNTs, Polypyrrole-CNT composite electrode material showed 85% of initial capacitance after five thousand

charging-discharging cycles in comparison to pure polypyrrole's retention of 66% of the

initial capacitance [41].
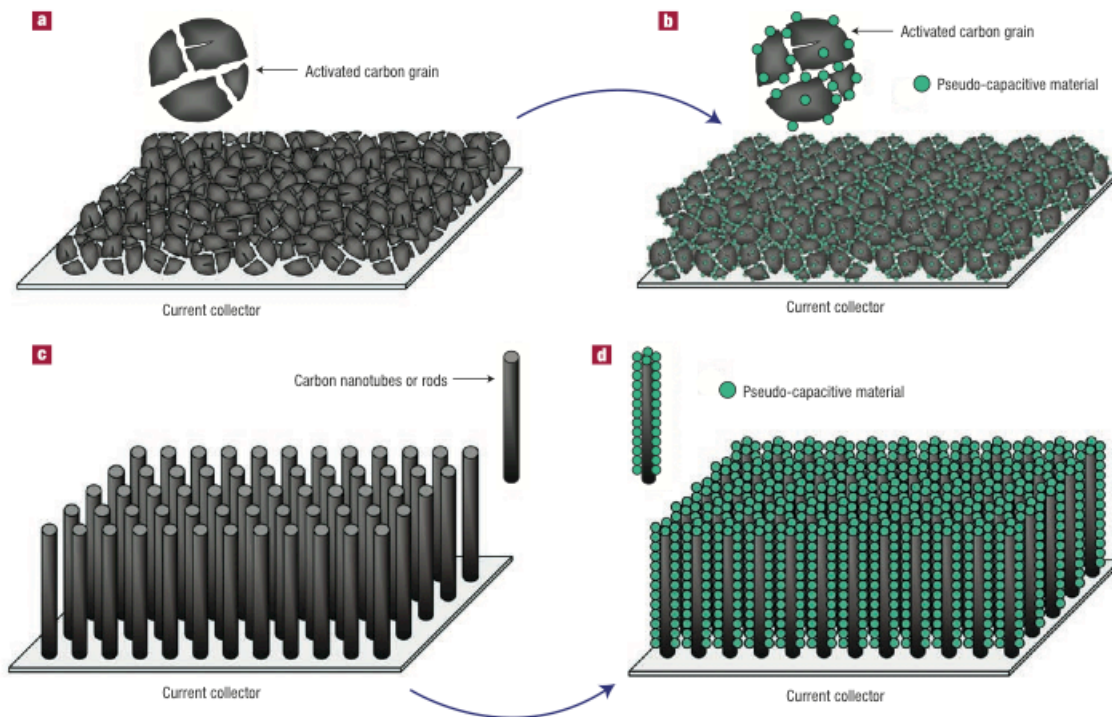
Fig 2-9 Possible strategies to enhance both energy and power densities for ESs: (a) carbon activation, (b) decorating with pseudocapacitive materials, (c) highly ordered high surface area carbon nanotubes (CNTs) and (d) deposit of pseudocapacitive materials onto CNTs [28]

MnO_2-CNT composites have a three-dimensional porous structure and are electric

conductive, which leads to an expanded potential range and higher utilization rate of

MnO_2 and CNTs [35, 37]. Since the potential range is related to the energy and power

densities of ES devices, the addition of CNT enables better performances of MnO_2 based

supercapacitors. According to Xia et al. [42, 43], MWCNT coated with MnO_2 reached a

capacitance as high as 210 F g^{-1} under a scan rate of 2 mV s^{-1}, which is nearly twice higher than pure MnO_2 with a capacitance of 110 F g^{-1}. Pure MnO_2 electrode only remained 25% of its initial capacity, but with the addition of CNT, the composite electrode achieved 77% of capacity retention [42].

Table 2-3 Summary of different types of supercapacitors [44]

Type of supercapacitor		Electrode material	Charge storage mechanism	Merits/shortcomings
Electrochemical double layer capacitor (EDLC)		Carbon	Electrochemical double layer (EDL), non-Faradaic process	Good cycling stability, good rate capability, low specific capacitance, low energy density
Pseudocapacitor		Redox metal oxide or redox polymer	Redox reaction, Faradaic process	High specific capacitance, relatively high energy density, relatively high power density, relatively low rate capability
Hybrid capacitor	Asymmetric hybrid	Anode: pseudocapacitance materials, cathode: carbon	Anode: redox reaction, cathode: EDL	High energy density, high power density and good cyclability
	Symmetric composite hybrid	Redox metal oxide/carbon or redox polymer/carbon	Redox reaction plus EDL	High energy density, moderate cost and moderate stability
	Battery-like hybrid	Anode: Li-insertion material, cathode: carbon	Anode: Lithiation/delithiation, cathode: EDL	High energy density, high cost and requires electrode material capacity match

Hybrid supercapacitors (Table 2-3) are made from different materials and they can be asymmetric hybrid supercapacitors made from different pseudocapacitive materials against carbon electrodes, symmetric composite hybrid supercapacitors with pseudocapacitive materials reinforced by CNTs and battery-like hybrid supercapacitors with Li-insertion materials and carbon electrodes. In composite materials, multiple charge storage mechanisms contribute to capacitive behavior of devices, which is beneficial for application of ESs.

2.5   Electrolytes for Electrochemical Supercapacitors

In conventional capacitors, dielectric materials are important, with which more charges can be stored. In electrochemical supercapacitors, electrolytes are essential because they can provide ions to form electrochemical double layers or help accomplish redox reactions that happen in pseudocapacitive electrode materials [9].

Since electrolytes play the role of charge mediators, their conductivity is of vital importance, which mainly depends on solubility of the electrolyte ions, mobility of free ions, dielectric constant of bulky solvent and viscosity of solvent [6]. Conway demonstrated an equivalent circuit model of single pore, which is shown in Figure 2-10. The liquid electrolytes can be classified into three categories: (a) aqueous electrolytes, (b)

organic electrolytes and (c) ionic liquids. Solid electrolyte and gel electrolyte are under

massive investigation as well [26, 45].
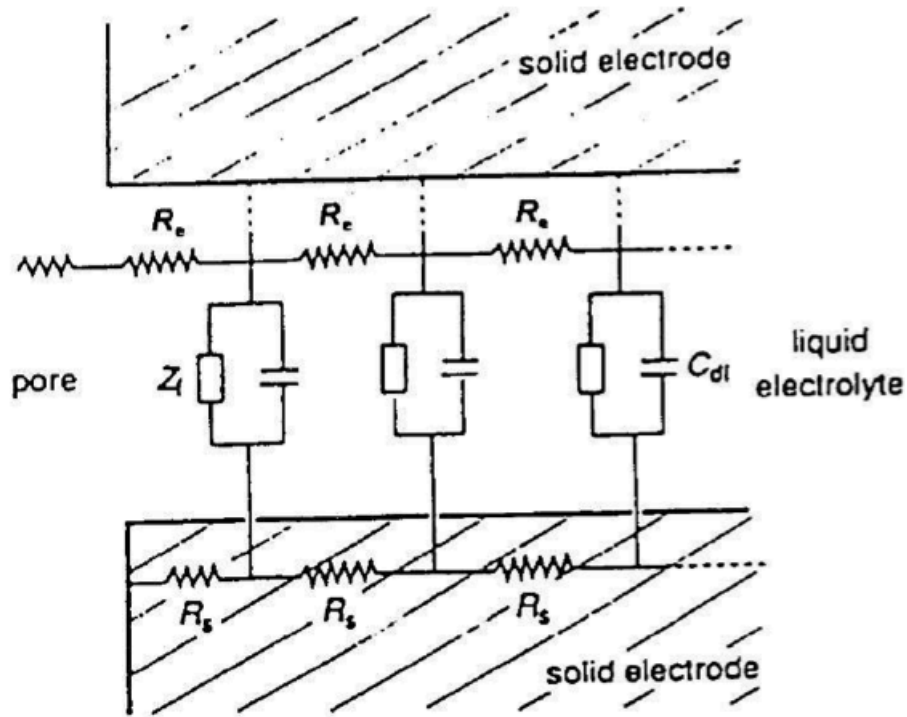
Fig 2-10 Transmission line model for a single pore [3]

2.5.1 Aqueous Electrolytes

Aqueous electrolytes can be acid solutions including H_2SO_4 and HCl [46], alkaline

solutions such as KOH and NaOH [47], and neutral salt solutions like $LiClO_4$, Na_2SO_4

and KCl [48]. It is said that aqueous electrolytes present higher ionic concentration and

lower resistance, which is beneficial for ES devices to obtain higher capacitance and

power density and it may be because of ionic radius is smaller in aqueous electrolytes. In

addition, aqueous electrolytes can be prepared in an easier way at lower costs and can be used under common conditions.

However, aqueous electrolytes have a drawback of a small potential window of only about 1.2 V [2], which strongly restricts the energy and power densities of the devices since voltage window plays an important role in achieving high energy and power.

2.5.2 Organic Electrolytes

Unlike aqueous electrolytes, organic electrolytes have a much larger voltage window reaching 3.5 V, which is the major advantage of organic electrolytes and higher energy density can be achieved than using aqueous electrolytes. Acetonitrile and propylene carbonate (PC) are most commonly used among organic electrolytes. More salts can be dissolved in acetonitrile than in other organic solvents, but it is at the cost of sacrificing environments and non-toxicity. PC, on the contrary, is environmentally friendly and can provide large voltage window and good electric conductivity [2]. However, most of organic solvents have a high resistance, which is 20 times higher than that of aqueous electrolytes [3], low solubility of ions leading to low power, complicated production and utilization conditions and high cost of fabrication.

2.5.3 Ionic Liquids

Ionic liquids (ILs) are molten organic salts that have low melting temperature and low

vaporization pressure with large potential window. ILs consist of pure cations and ions and ionic liquids often have better electric conductivity at higher temperatures. Their potential window is determined by electrochemical stability of ions [49].

2.6 Fabrication Methods of Electrode based on Conducting Polymer

CPs are under intensive research now and the most commonly used CPs are Polypyrrole (PPy), Polyaniline (PAni), Polythiophene (PTh) and their corresponding derivatives [19]. CPs have a lot of advantages, including high theoretical specific capacitance, high electric conductivity, high charge density, lower equivalent resistance and low fabrication cost [19].

2.6.1 Electrochemical Properties of Conducting Polymers

Physical and electrochemical properties of CPs vary from each other due to different elements and synthesis approaches. The chemical structures of commonly used CPs and derivatives are shown in Fig 2-11.
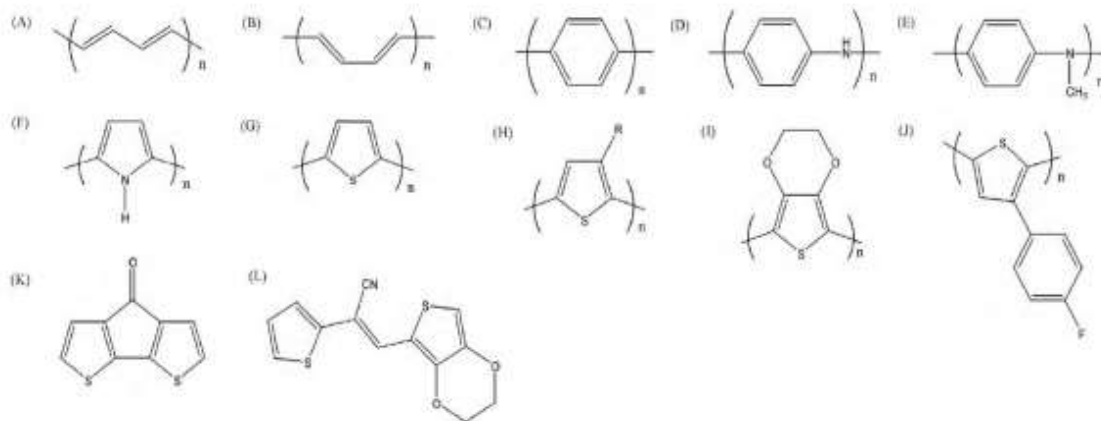
Fig 2-11 Chemical structures of commonly used CPs or monomers.

(A) trans- and (B) cis-poly (acetylene), (C) poly(p-phenylene), (D) polyaniline (PAni),
(E) poly(n-methylaniline), (F) polypyrrole, (G) polythiophene, (H) 3-substituted
polythiophene, (I) poly(3,4- ethylenedioxylthiophene), (J)
poly(3-(4-fluorophenyl)thiophene), (K)
poly(cyclopenta[2,1-b;3,4-b'-dithiphen-4-one]), (L) 1-cyano-2-(2-[3,4-
ethylenedioxylthienyl]-1-(2-thienyl)vinylene)[19].

Conductivity of CPs can be enhanced in the doped state and it is dependent on doping

level, mobility of charge carriers, chemical environment (bulk or solution) and doping

temperature [50]. Among common CPs in application of ESs, PAni and PPy can only be

p-doped because the n-doping potential is much lower than the reduction potentials of

commonly used electrolytes. All CPs have certain working potential window, and if the

potential is beyond a strict potential window, the CPs may be degraded at more positive

potentials and at more negative potentials, CPs may be changed into an insulating state

[19].

Among CPs, PPy offers better flexibility than most other ones, which makes PPy under intensive investigation and PPy has become the subject of a lot of research efforts concerning ESs. PPy has a theoretical capacitance as high as 620 F g^{-1}. It can only be p-doped with dopants that are negatively charged ions, such as typical single valent ions including Cl$^-$, ClO$_4^-$ and SO$_3^-$. However, if doped with multiple valent dopants, interlinks between different polymer chains may be formed, which will lead to the increase in capacitance due to higher conductivity and porosity of the material [19].

2.6.2 Synthesis of Polypyrrole

PPy is a promising conducting polymer with relatively high theoretical capacitance and conductivity. It can be synthesized both by chemical and electrochemical methods. Both of them share the same mechanism, which is shown in Fig 2-12, but oxidants are needed in chemical synthesis process.
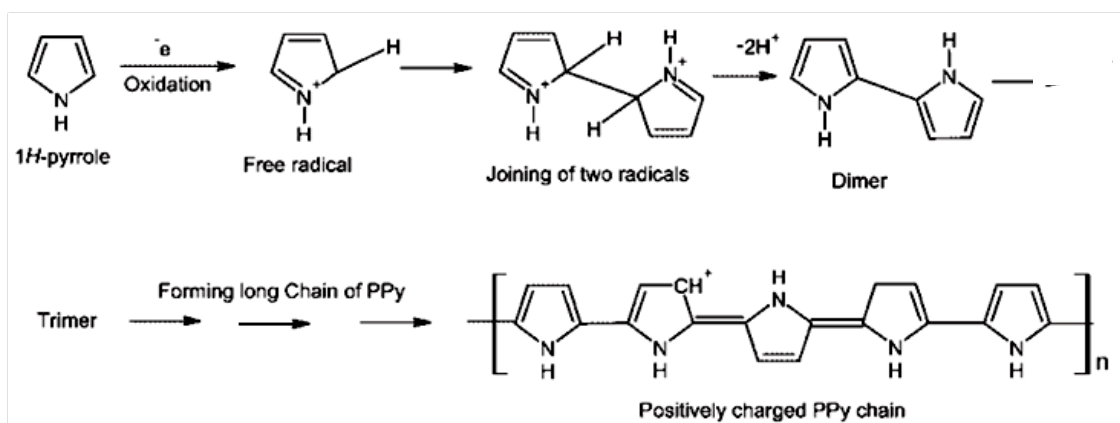
Fig 2-12 Mechanism of synthesis of PPy [6]

In this process, pyrrole monomer is first oxidized and gives up an electron, generating a free cation radical. And then, two radicals combine together and form a dimer. Free radicals keeps joining in as the process goes on and eventually a PPy chain is obtained. The first two steps are fairly important, which controls the synthesis time [51]. However, since PPy polymer has a lower oxidation potential than monomers, the oxidation of PPy polymer chain happens along with the synthesis process and two reactions happen simultaneously, leading to the production of positively charged PPy polymer [19].

2.6.2.1   Chemical Synthesis

The product of chemical synthesis of PPy is black powders and its advantages include high production rate, easy and stable synthesis process, controllable mass loading of electrodes and capability to modify of PPy polymer morphology.

In chemical synthesis of PPy, oxidants are needed and have a great influence on the morphology of PPy [40]. Commonly used oxidants are peroxydisulfate anions ($S_2O_8^-$), ferric cations (Fe^{3+}), and copper cations (Cu^{2+}) [52, 53]. Under acidic conditions, oxidants such as ferrous cations (Fe^{2+}) [54], permanganate (MnO_4^-) [55], dichromate ($Cr_2O_7^{2-}$) [56] can also be used for synthesis of CPs. During chemical polymerization process, dopants for PPy and oxidants influence morphology and capacitive behaviors of PPy, and especially the conductivity of PPy, as given by Table 2-4. Clearly we can see that with the utilization of oxidants containing iron cations, a high conductivity can be

achieved, it may be because that a part of iron cations contribute to conductivity of PPy powders. Ammonium persulfate is another promising candidate for chemical synthesis and is utilized in this research.

Table 2-4 Various oxidants for PPy chemical polymerization [53]

Oxidant (mol dm^{-2})	Additive (mold m^{-2})	Yield (g)	Conductivity (S cm^{-1})
$(NH_4)_2S_2O_8$ (0.1)		1.36	4.42
$(NH_4)_2S_2O_8$ (0.1)	NaDBS (0.0225)	2.01	0.570
$(NH_4)_2S_2O_8$ (0.1)	NaANS (0.024)	1.91	0.221
$Fe_2(SO_4)_3$ (0.1)		1.28	1.33
$Fe_2(SO_4)_3$ (0.05) $(NH_4)_2S_2O_8$ (0.05)	NaDBS (0.0225)	2.46	20.4
$Fe_2(SO_4)_3$ (0.1)	NaDBS (0.0225)	2.44	26.1
$Fe_2(SO_4)_3$ (0.1)	NaANS (0.024)	2.65	15.7
$Fe_2(SO_4)_3$ (0.1)	NaAS (0.022)	2.24	40.7

2.6.2.2   Electrochemical Synthesis

Electrochemical polymerization has been widely used for PPy thin film sample making and has been under intense investigation. It has a lot of advantages including in-situ simultaneous polymerization at substrate surface and ease to control film thickness and composition by modifying parameters such as deposit current density and concentrations

of composition.

Unlike chemical synthesis, it is not necessary to add oxidants in solutions ready for

deposition because the reaction is emerged by electric current. There are various ways for

deposition, such as potentiostatic deposition (with constant potential) [57], galvanostatic

deposition (with constant current) [58], potentiodynamic deposition [59] and pulse

electro-deposition [60, 61]. Usually we choose the constant current density power source

for deposition over the constant potential deposition, because with the increase in the film

thickness, resistance of the deposit increases, which leads to difficulties in ions attracting

to the substrate and deposit. Among these four methods, pulse electro-deposition is

considered the best way to deposit uniform PPy thin films.
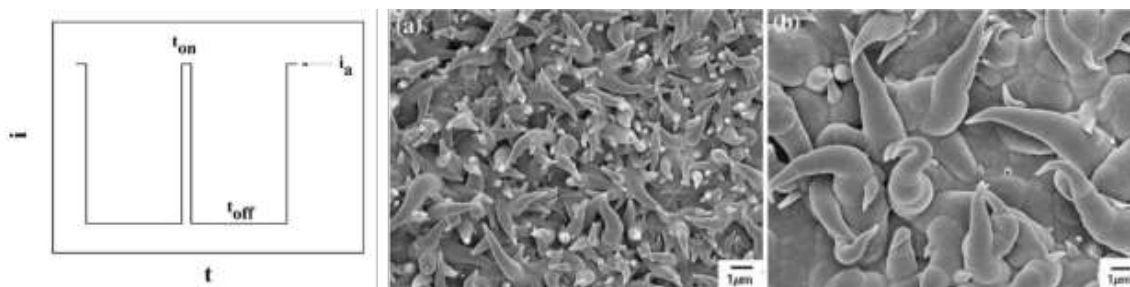
Fig 2-13 Sketch of mechanism of pulse electrochemical deposition (t_{on} is time for

deposition and t_{off} is rest time). (a) is the SEM image of pulse electrochemical deposited

PPy and (b) is the SEM image of galvanostatic deposited PPy [62]

The structure of deposited PPy thin film depends strongly on applied current density [63].

For electrochemical synthesis, Py monomers and additives are dissolved in a solution and consumed on electrode surface. At the interface of electrode and electrolyte, a concentration gradient exists and that is the driving force for attracting monomers and additives to the substrate surface. Diffusion takes a longer time than polymerization, which leads to defects occurring in uniform thin films [64]. However, with pulse electrochemical deposition method, when rest time begins, sufficient time is given for monomers to diffuse from the solution to electrode surface and thus, uniform PPy thin films can be obtained, which can be clearly seen from SEM comparisons between the two samples.

However, it is challenging to use PPy thin films for practical applications mainly due to three reasons. Firstly, unlike the product of black PPy powders of chemical synthesis, thin films are difficult to remove from substrates for further testing. If deposited PPy films on substrate are directly used, the capacitance would be lower because of non-contributing components. Other reactions like substrate dissolution or reactions between substrate and other components in electrolyte may affect polymerization and ultimate capacitance results. Secondly, conductivity of PPy films decreases along with the increase of film thickness, which makes it difficult to obtain thick films and high mass loading on substrate. And thirdly, PPy thin films on substrate show adhesion problem during cycling due to film swelling and shrinkage, which leads to increased

impedance and shorter cycle life [3].

2.6.3 Functions of Dopants

Anionic dopants are of vital importance and they can affect greatly the morphology and capacitive properties of PPy films and powders in many ways.

During electrochemical synthesis of PPy, dopants can help to passivate the surface of non-noble metal and reduce or prevent substrate dissolution. Adherent films can be obtained on stainless steel substrate from solutions containing oxalate [65]. However, a non-conductive and non-capacitive layer of iron oxalate may form and increases the resistance of charge transfer and reduce the total capacitance of PPy films (Fig 2-14).

Fig 2-14 The formation of iron oxalate layer [66]

However, aromatic dopants can act as charge transfer mediators. For example, Tiron can reduce the deposition potential of PPy and lower the possibility of metal dissolution (like

shown in Fig 2-15) without the formation of resistant iron oxalate layer.

Dopants also have great influence on conductivity of PPy films and powders. With the usage of aromatic dopants, preferred orientation of polypyrrole ring parallel to the electrode or growth surface [67] and anisotropic film growth can lead to increased conductivity. In chemical synthesis, aromatic dopants with multiple charged groups, interlinks between different PPy polymer chains and increase the mobility of charge carriers, thus enhance conductivity. Conductivity properties of PPy doped with various dopants are shown in Table 2-5, where with dopants possessing larger molecular mass and higher charge-mass ratio, the conductivity of PPy increases.
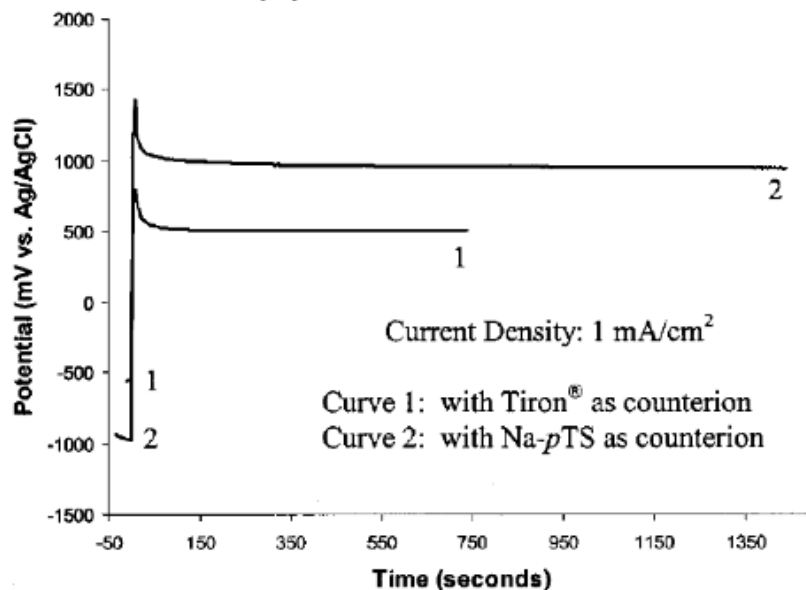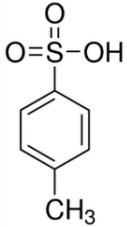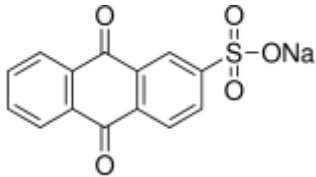
Fig 2-15 Deposition potential vs. time in two solutions containing Tiron (curve 1) and Na-pTS (curve 2), respectively [66]

Table 2-5 Examples of conductivity figures of PPy doped with different dopants[66]

Dopants	PPy-Cl⁻	PPy-HSO₄⁻	PPy-TS⁻	PPy-AQS⁻
Conductivity σ (S/cm)	1.59	3.08	7.10	120
Molecular formula or structure	$FeCl_3$	$(NH_4)_2S_2O_8$		

Dopants can also affect the structure of PPy. With larger molecular size, dopants are considered more like "fixed" molecules and when connected to PPy polymers, they help to reduce movement during charge-discharge cycles and PPy shrinkage or swelling, which leads to enhanced cyclic stability. However, on the other hand, larger sized dopants restrict the doping level and to some extent, restrains the conductivity of doped PPy.

2.6.4 Dispersions of MWCNTs using surfactants

MWCNTs have unique properties that position them for a wide scope of applications, including high mechanical stability, excellent electric conductivity, high aspect ratio (length to diameter ratio), etc. The addition of MWCNTs into PPy matrix will enhance not only mechanical stability, but also conductivity. However, it is a challenge to obtain homogeneous MWCNTs suspension because of their high surface area that increases the

possibility of MWCNTs to agglomerate. And efforts have been invested into developing

methods for MWCNT dispersion and so far there are mainly two kinds, mechanical

method and chemical method. Mechanical methods refer to ball milling, ultrasonication,

high shear mixing and so on [68]. They are way less effective than chemical methods and

may cause break of MWCNTs into fragments, which lowers the aspect ratio and

sacrifices other properties. Chemical methods, however, work better for dispersing

MWCNTs. They can be divided into two categories, covalent functionalization and

non-covalent functionalization [31].

Covalent functionalization is to provide needed groups onto the MWCNT scaffold. It can

be direct covalent functionalization, which can be accomplished by using molecules of

high chemical activity like fluorine. It is associated with a change of hybridization from

sp^2 to sp^3 and a simultaneous loss of p-conjugation system on a graphene layer. It can

also be defect functionalization with the usage of strong acids or oxidants. Once the

defects are formed on MWCNT scaffold, MWCNTs can be stabilized by bonding with

certain groups. However, covalent functionalization, to some degree, damages the

structure of MWCNT and thus sacrifices their chemical properties. Thus non-covalent

functionalization is preferred. As for non-covalent functionalization, it is pure physical

adsorption of molecules onto MWCNTs through van der Waals and/or π-π stacking and

the molecules can be polymer chains or surfactants. Fig 2-16 represents how surfactants

are adsorbed onto MWCNTs.
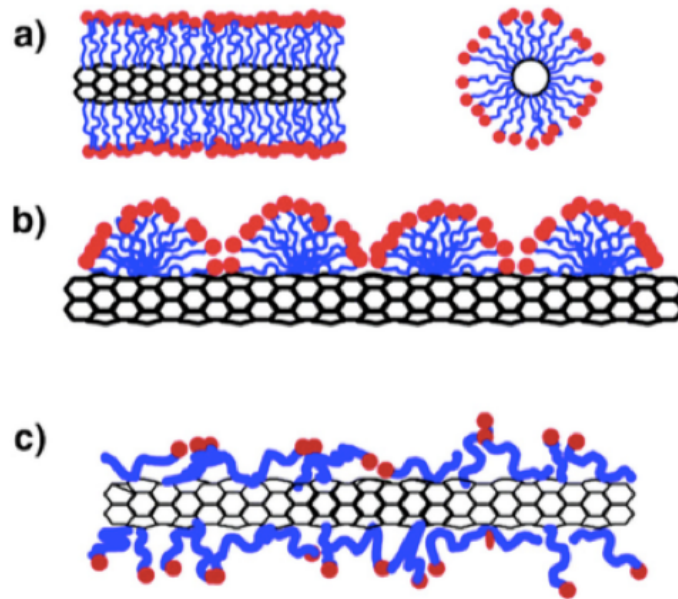
Fig 2-16 Sketch of head-tail surfactants adsorption onto MWCNTs [31]

After surfactants are adsorbed onto MWCNTs, ultrasonication for minutes can help separate single MWCNT from carbon nanotube bundles. Once a gap at the bundle end is formed, surfactants can penetrate in and separate MWCNTs through static or electrostatic repulsions (Fig 2-17).
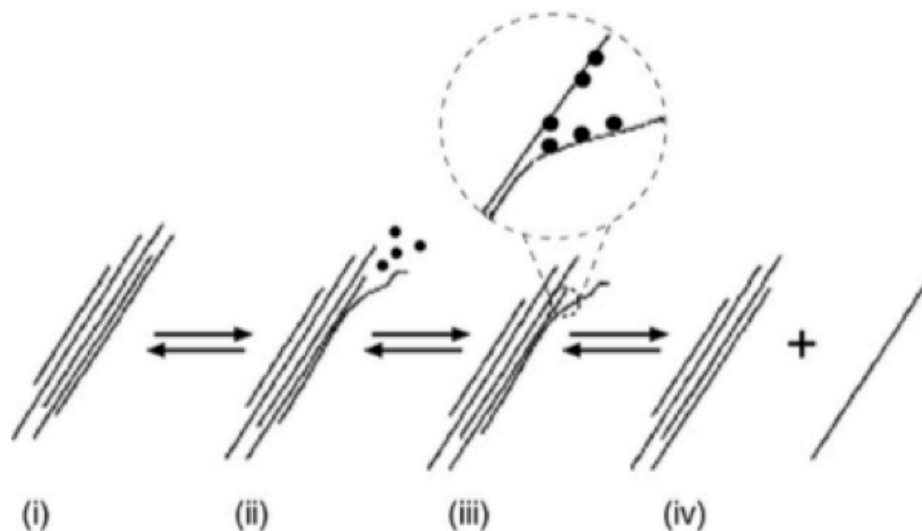
Fig 2-17 Sketch of mechanism of dispersing MWCNT using surfactants [31]

3 Problem Statements and Objectives

Advanced dopants have great influences on morphology and capacitive properties of PPy and PPy/MWCNT composite materials. And we are looking for advanced dopants with high charge to mass ratio, large molecular size and polyaromatic structures. And to synthesize composite materials, the dispersion of MWCNT is a challenging step because it has high aspect ratio that enhances the possibility of agglomeration, which makes the selection of dispersing agent of vital importance. For electrochemical deposited samples, adhesion issue relates directly to the testing results. As a result, problems that have been encountered in this research include selection of advanced dopants, dispersion of MWCNT and adhesion of PPy thin films on non-noble metal substrates during electrochemical synthesis.

The overall objective of my thesis work is to develop advanced electrode materials for electrochemical supercapacitors and it includes the following:

- Optimizing selection of advanced anionic dopants for PPy thin films and powders and investigate the influence of dopant structure on PPy.

- Developing novel dispersing agents for MWCNT to synthesize composite materials and multifunctional dopants that can act as dispersant and dopant at the same time.

- Developing films with high adhesion and enhanced capacitive property.

4 Approaches and Methodology

4.1 Approaches

PPy powders are synthesized by chemical polymerization process with the presence of anionic dopants and oxidant Ammonium persulfate ($(NH_4)_2S_2O_8$, APS). The product is then studied for morphology and fabricated as an electrode for capacitive tests. PPy thin films are deposited onto stainless steel substrate by electropolymerization from monomer solutions, containing anionic dopants.

Multi-walled carbon nanotubes (MWCNTs) are incorporated into PPy matrix to enhance

mechanical and electrochemical properties. The composite materials are synthesized and

studied in the same way for pure polypyrrole material by adding well dispersed MWCNT

to the pyrrole solutions.

4.2 Methodology

4.2.1 Dopants for doping PPy

Dopants' structures have a strong influence on capacitive behaviors of electrode materials.

It was found that dopants with large molecular size, high charge-mass ratio and aromatic

rings are preferred. Fig 4-1 and Fig 4-2 show chemical structures of dopants and

multifunctional dopants used in this research.
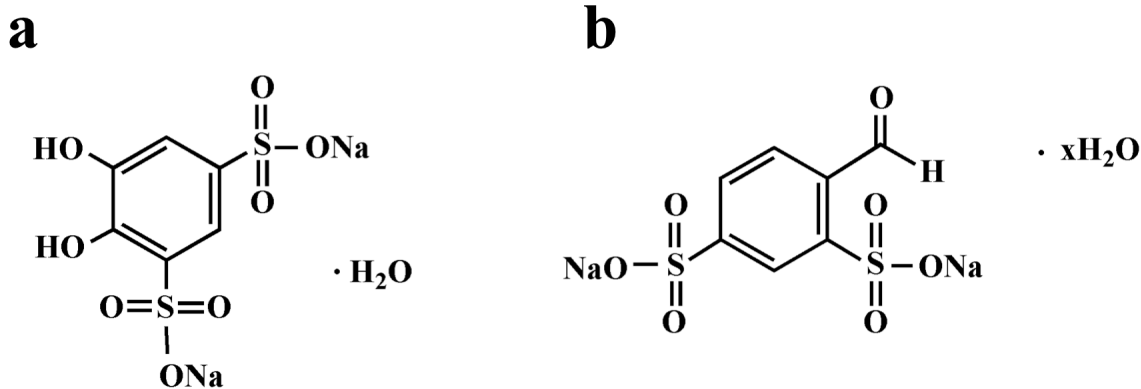
Fig 4-1 Chemical structures of dopants for Pyrrole.
a is 4,5-Dihydroxy-1,3-benzenedisulfonic acid disodium salt monohydrate (also known as Tiron); b is 4-Formylbenzene-1,3-disulfonic acid disodium salt hydrate (FDS)
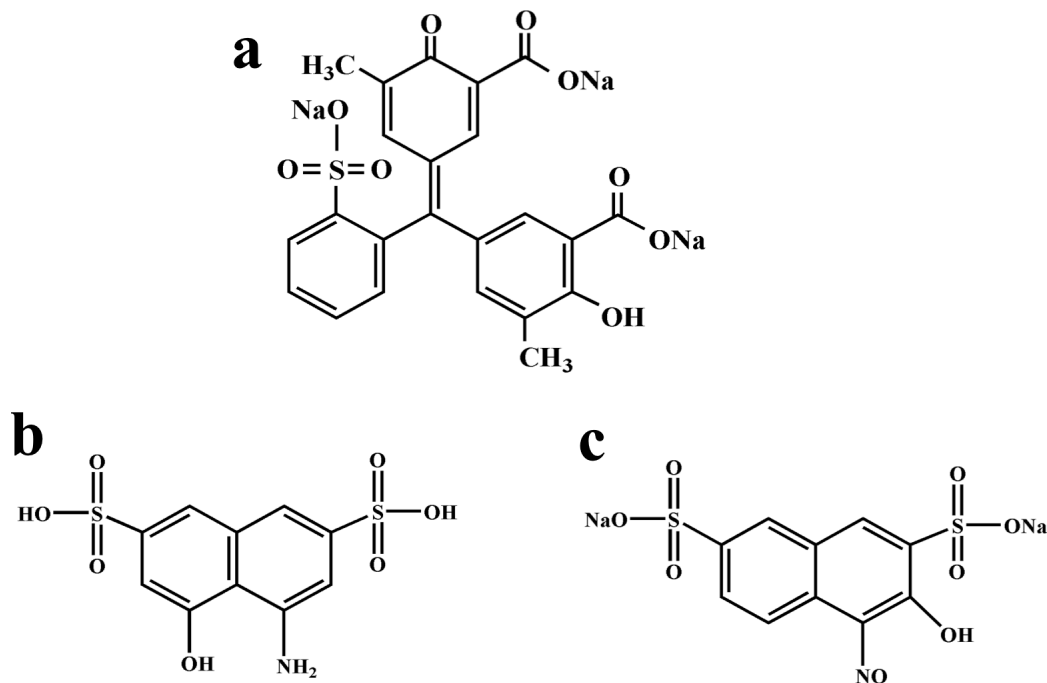
Fig 4-2 Chemical structures of multifunctional dopants.
a is Eriochrome Cyanine R (ECR); b is 4-Amino-5-hydroxy-2,7-naphthalenedisulfonic
acid monosodium salt hydrate (AHN); c is
3-Hydroxy-4-nitroso-2,7-naphthalenedisulfonic acid disodium salt (HNN)

Dopants mentioned above are soluble in water and can act as anionic dopant for Pyrrole.

And also, they have large molecular size and high molecular mass with multiple charged

groups. Results of electrochemical behavior will be discussed in details in Chapter 6.

4.2.2 Advanced PPy-CNT Composites

Uniform dispersion of CNT in PPy matrix will not only reinforce polymer backbone, but

also enhance conductivity of the composite material. Fig 4-3 presents the molecular

structure of dispersing agents studied in this research.
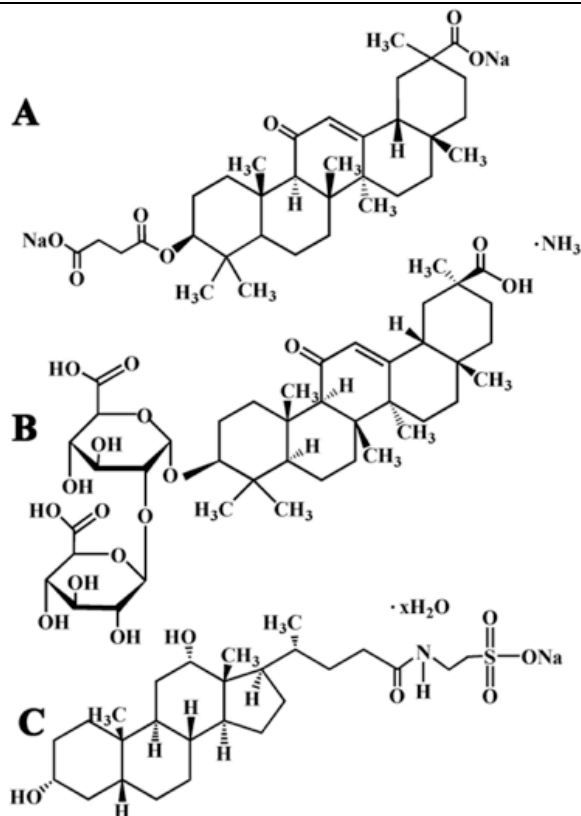
Fig 4-3 Chemical structures of three dispersing agents for CNTs. A is carbenoxolone disodium salt (CXNa$_2$); B is glycyrrhizic acid ammonium salt from glycyrrhiza root (GANH$_3$, also known as Licorice); C is sodium taurodeoxycholate (TDNa)

With these dispersants, CNT suspension can be stable up to several months and multifunctional dopants can act as advanced dispersing agents for CNT for the fabrication of composite materials.

5 Experimental Procedure

5.1 Materials Preparation

All materials involved in this research are listed in Table 5-1.

Table 5-1 Materials involved in this research

| Category	Chemical Name	Source
Monomer	Pyrrole (Py) (> 98%)	Sigma Aldrich (CA)
Oxidant	Ammonium Persulfate (APS)	
Dopants	4, 5-Dihydroxy-1, 3-benzenedisulfonic acid disodium salt monohydrate (Tiron)	
	4-Formylbenzene-1, 3-disulfonic acid disodium salt hydrate	
Multifunctional Dopants	Eriochrome Cyanine R (ECR)	
	4-Amino-5-hydroxy-2,7-naphthalenedisulfonic acid monosodium salt hydrate (AHN)	
	3-Hydroxy-4-nitroso-2,7-naphthalenedisulfonic acid disodium salt (HNN)	Fluka (CA)
Dispersants	Carbenoxolone disodium salt (CXNa$_2$)	Sigma Aldrich (CA)
	Glycyrrhizic acid ammonium salt from glycyrrhiza root (GANH$_3$)	
	Sodium taurodeoxycholate (TDNa)	
Additive	Multi-walled carbon nanotubes (MWCNTs)	Bayer Inc. (CA)
Electrolyte salt	Sodium sulfate (Na$_2$SO$_4$)	Sigma Aldrich (CA)
Other chemicals	Poly (vinyl butyral-co-vinyl alcohole-co-vinyl acetate) (PVB)	Aldrich Chemical
	Ethanol	Greenfield Alcohol Inc.
Current collectors	Nickel foam (porosity ~95%)	Vale (CA)
	Stainless steel foil	Alfa Aesar

5.2 Chemical Synthesis of PPy and PPy-CNT Composite Materials

To synthesize PPy powders (Fig 5-1 (a)), the first step is to dissolve Py monomer with dopants in deionized water and to stir continuously during experiment in ice bath (about 4 °C). After that, mix solutions containing APS and Py monomer and dopant together. Reaction begins after mixing and should be kept at low temperature around 4 °C. Reactions take at least four hours to complete and for the first two hours, the solution should be processed with ultrasonication or magnetic stirring. After the final suspension with PPy powders is obtained, vacuum filtration with filter paper are used to separate powders and excess dopants and oxidants. The powders should be kept in oven for at least 24 hours at 60 °C to dry out.
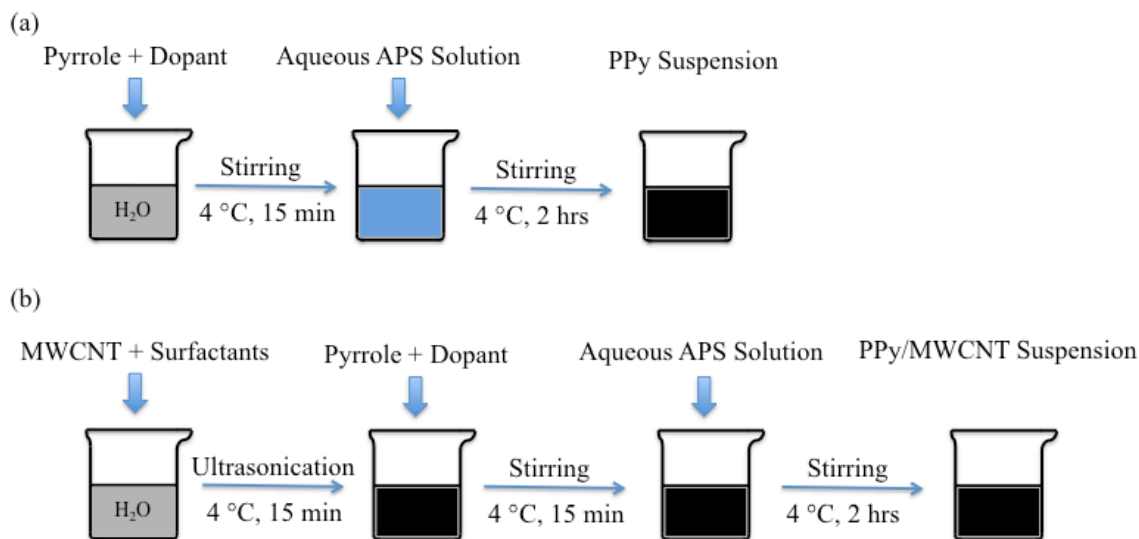
Fig 5-1 Sketch of chemical synthesis procedure. (a) synthesis of pure PPy powders; (b) synthesis of composite materials

To synthesize PPy-CNT composite materials (Fig 5-1 (b)), MWCNTs should be dispersed first, and then Py monomer and dopant were added into the uniform CNT suspension. Other procedures are the same as the rest of PPy synthesis procedure. For dispersion of MWCNTs, surfactants should be dissolved in deionized water or ethanol first. Then add MWCNT to the solution and keep ultrasonication for at least 15 minutes.

5.3 Electrochemical Synthesis of PPy (/MWCNT) thin films

The electrochemical synthesis of PPy and PPy-CNT thin films was accomplished by a set up shown in Fig 5-2. Similar to the chemical synthesis process, MWCNTs should be well dispersed and Py monomers and corresponding dopants should be dissolved first and kept at low temperature. Then the electrode system is inserted in the suspension or solution with the stainless steel electrode in the middle connecting to positive electrode of external

power source and platinum foils connected to negative electrode of external power source.

And PPy or PPy-CNT composite films are deposited on the stainless steel foil.
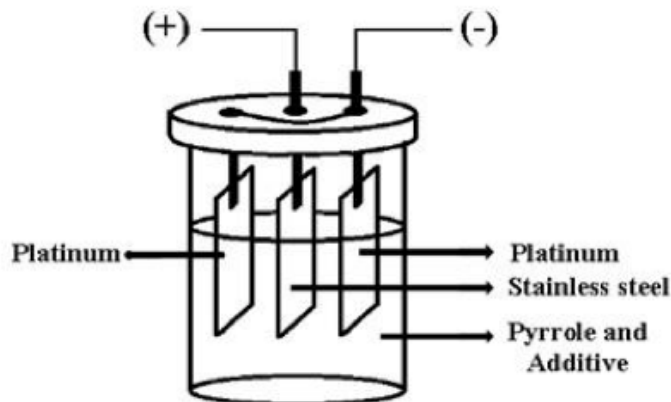
Fig 5-2 Sketch of set up for electrochemical synthesis of deposited samples [66]

5.4 Fabrication of Electrodes

To obtain powders, the PPy and composite PPy-MWCNT material suspensions need to

be filtrated with filter papers or vacuum filtration. With filter papers, there may be more

powders left on the paper, which leads to unnecessary waste. During filtration, the

materials must be washed with 1 L water and 500 ml ethanol in order to remove excess

additives and oxidant. After that, the PPY or composite PPy-MWCNT powders must be

dried in oven at 60 °C temperature for at least 24 hours.

To fabricate PPy and composite powders into electrodes ready for electrochemical testing,

the powders should be ground in a mortar first with ethanol and with PVB as a binder.

PVB is better dissolved in ethanol first to be fully utilized and functional. When grinding,

add a few drops of ethanol at a time to make a slurry. After weighing a clean piece of Ni

foam, paste the slurry onto the nickel foam and the powders penetrate inside the pores of

the Ni foam. The working area of an electrode is 1 cm^2 and active material is pasted on

both sides. The electrode surface should be full covered with PPy powders without any

exposure of Ni. Put away the pasted Ni foam for drying, followed by weighing again to

calculate the mass of active materials. And then, use a rolling machine to reduce the

thickness of the pasted Ni foam to 30% of its original thickness (around 2 mm), which

helps powders impregnate into the Ni foam (Fig 5-3). As for electrochemical deposited

samples, the stainless steel substrates with thin PPy or PPy/MWCNT films on them are

cut in a circle with a diameter around 1.2 cm and it is kept in a sample holder when

testing. All electrochemical tests are done using a three-electrode system with Na$_2$SO$_4$ as

electrolyte and platinum gauze as counter electrode.
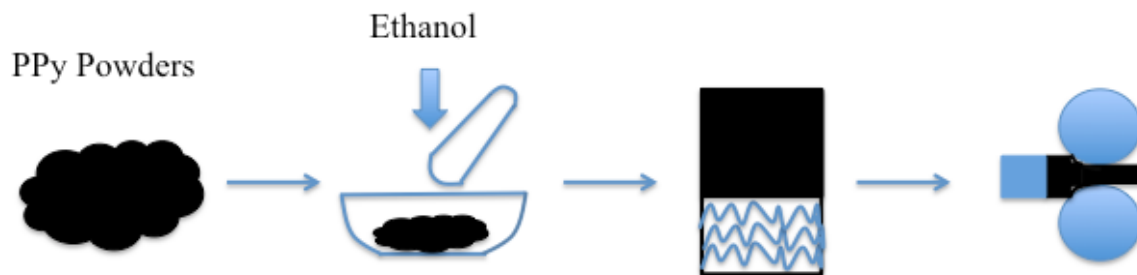
Fig 5-3 Sketch of fabrication of electrode for electrochemical testing

5.5 Characterization

5.5.1 Morphology Characterization

The morphology of PPy powders from chemical synthesis and PPy thin film from electrochemical polymerization and composite materials is characterized by JEOL JSM-700F Scanning Electron Microscope (SEM) under magnification from 5,000-50,000X and FTIR (spectrometer FTS-40, Bio-Rad).

5.5.2 Electrochemical Characterization

Electrochemical tests include Cyclic Voltammetry (CV) and Electrochemical Impedance Spectroscopy (EIS) were conducted using a PATSTAT 2273 Potentiostat from Princeton Applied Research.

Capacitances under different scan rates can be calculated from CV curves using the following equation,

$$C_m = \frac{A}{2mv(V_{max}-V_{min})} \qquad \text{5-1}$$

where A is the integrated area of CV curve, m is mass of active materials on current collector, v is scan rate and (V_{max}- V_{min}) is the working potential window of PPy (which

is 0.9 V).

A small amplitude of 5 mV of alternating voltage is applied in the EIS investigation in the frequency range of 10 mHz to 100 kHz. Impedance can be expressed in complex form $Z^* = Z' - iZ''$. The complex form of capacitance is expressed as following, $C^* = C' - iC''$ and can be calculated from the following equations,

$$C' = \frac{Z''}{2\pi f |Z|^2}$$
<div align="right">5-2</div>

$$C'' = \frac{Z'}{2\pi f |Z|^2}$$
<div align="right">5-3</div>

where f is the testing frequency and Z equals to $\sqrt{(Z')^2 + (Z'')^2}$ [69].

6 Results and Discussion

6.1 Polymerization of PPy/MWCNT Composite Materials with Different Dispersants

In order to understand the function of dispersing agents and optimize the selection of chemicals, three dispersants including Carbenoxolone disodium salt ($CXNa_2$),

Glycyrrhizic acid ammonium salt from glycyrrhiza root ($GANH_3$) and Sodium taurodeoxycholate (TDNa) were under investigation. The chemical structures of these three chemicals are shown in Fig 4-3. The selected molecules have steroid-like structures with hydrophilic and hydrophobic groups. $CXNa_2$ is a derivative of the glycyrrhetinic acid, containing two anionic carboxylic groups. The hydrophilic and anionic properties of $GANH_3$ are related to two glucuronic acid groups and a carboxyl group, whereas methyl groups impart hydrophobic properties to the $GANH_3$ molecules. TDNa is an anionic molecule, containing negatively charged SO_3^- group. The amphiphilic structure of TDNa is defined by the hydrophilic OH groups on the concave surface and the hydrophobic methyl groups on the convex surface. In contrast to head-tail surfactants, the selected molecules do not have flexible alkyl chains.

6.1.1 Sedimentation Test and Morphology Characterization

In order to get uniform and stable MWCNT suspension, dispersants were first dissolved in water and after the addition of MWCNTs, ultrasonication was applied for at least 15 minutes. The sedimentation results are shown in the following figure (Fig 6-1) where A is 1 g L^{-1} MWCNT in water after ultrasonication. MWCNT in suspensions, prepared without dispersants, precipitated in a short time. On the contrary, B, C and D sample are MWCNTs with dissolved $CXNa_2$, $GANH_3$ and TDNa, respectively after ultrasonication. The suspensions, containing dispersants, were stable for months. Among these three, TDNa gave the best performance and the suspension remained stable for 12 months. The

negatively charged CX^{2-}, GA^- and TD^- species adsorbed on CNT due to the hydrophobic

interactions and provided electrostatic dispersion of CNT.
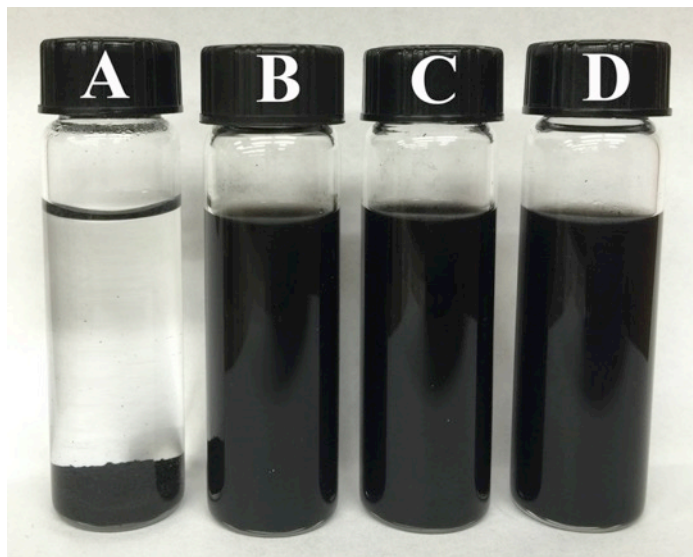
Fig 6-1 Sedimentation results comparison: 1 g L^{-1} suspensions of CNT: (A) without
dispersant and containing (B) 1 g L^{-1} $CXNa_2$, (C) 1 g L^{-1} $GANH_3$ and (D) 1 g L^{-1} TDNa.

In the investigation of dispersing agents for MWCNT, 4, 5-Dihydroxy-1,

3-benzenedisulfonic acid disodium salt monohydrate (Tiron) was used as anionic dopant

for Py monomer. During electrochemical deposition process, PPy was deposited on

stainless steel substrate and Fig 6-2 presents the spherical morphology of PPy with

average particle size less than 2 μm. Different concentration of Tiron were investigated

and with molar ratio of Py to Tiron 20 to 1, black and shinny thin films were obtained

and the concentration of Py and Tiron were finalized at 0.2 mol L^{-1} and 0.01 mol L^{-1},

respectively.
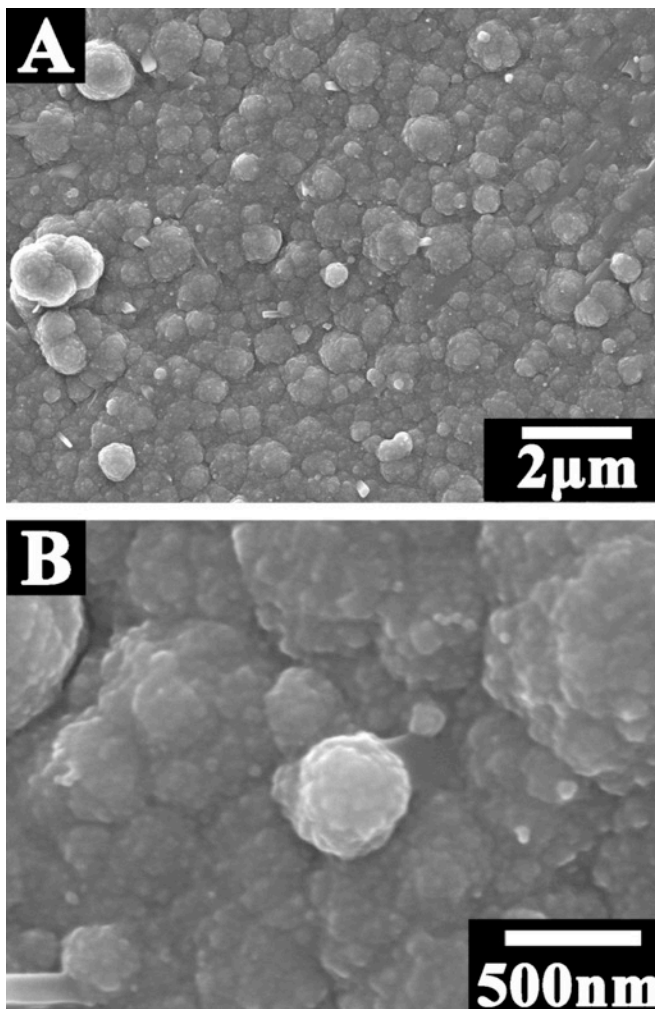
Fig 6-2 SEM images of PPy films, deposited at current density of 10 A m^{-2} for 8 min from 0.2mol/L Py and 0.01mol/L Tiron solution

In order to electrochemically synthesize composite materials, deposition of MWCNT with dispersants were conducted prior to deposition of PPy coated MWCNT. Among these three chemicals, CXNa$_2$ can deposit itself in a large amount, shown in Fig 6-5 A, which means that once the composite materials are synthesized with the chemical, the self-deposit may influence the final capacitive results.

Thin films of pure $CXNa_2$ were obtained from 0.5-3 g L^{-1} $CXNa_2$ solutions by anodic electrodeposition at a current density of 10 A m^{-2}. The slope of the deposit mass versus $CXNa_2$ concentration dependence increased, deviating from the linear Hamaker's law. The mechanism of deposition involved the anaphoresis of anionic CX^{2-} species, their discharge and film formation at the anode. The electrochemistry of film formation involved H^+ generation at the anode in the reaction:

$$2H_2O \rightarrow 4H^+ + O_2 + 4e^-$$ 6-1

The protonation of the CX^{2-} species resulted in the formation of the acidic form of carbenoxolone, which has low solubility in water:

$$CX^{2-} + 2H^+ \rightarrow CXH_2$$ 6-2

The deviation from the Hamaker's law can be explained [70] by the shift of the film-solution interface during the deposition, which must be taken into consideration. In this case the deposit mass (M) is given by the equation

$$M = \mu EtSC_sC_c/(C_c-C_s)$$ 6-3

where μ is electrophoretic mobility, S- substrate area, E–electric field, t-deposition time, C_c is the CXH_2 concentration in the film, C_s is the $CXNa_2$ concentration in the solution. The Hamaker's law can be obtained when $C_c >> C_s$.

The deposit mass of MWCNT with $CXNa_2$ versus time dependence at a constant current density was nearly linear and showed a continuous mass gain due to the film formation (Fig 6-3 B). The films, prepared by electrodeposition were studied by SEM. Fig 6-3 C and D show SEM images of the films at different magnifications. Deposition resulted in continuous and dense films, which were crack free. The SEM images showed a flaky morphology of the films.
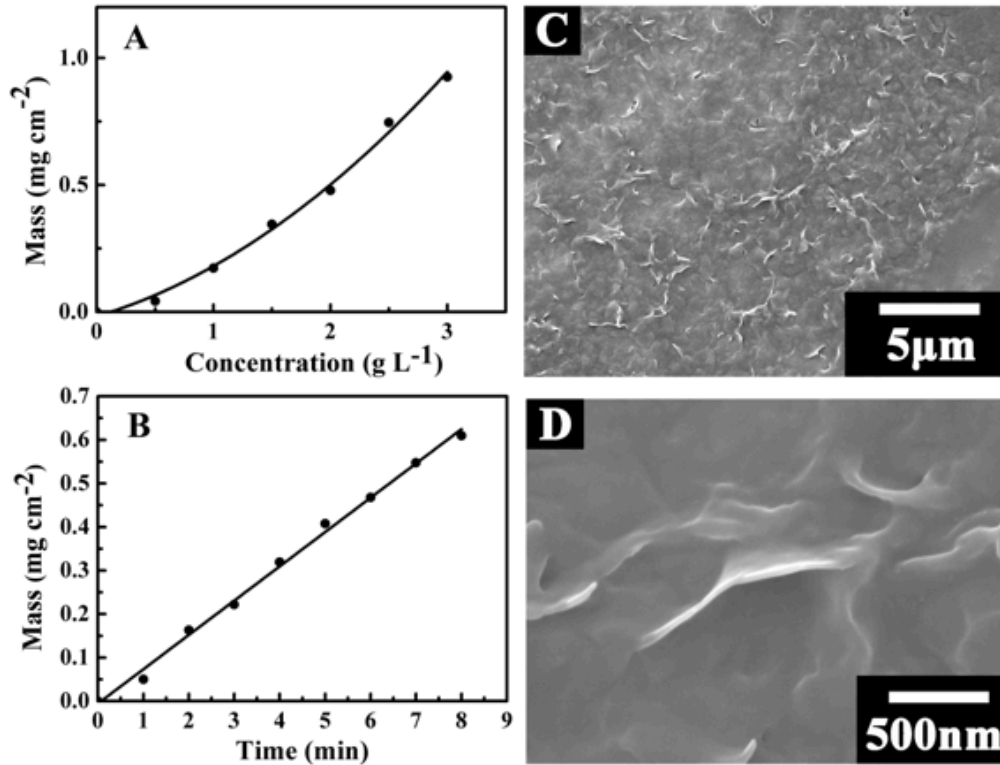
Fig 6-3 A. deposit masses vs. concentrations of CXNa$_2$ curve at 10 A m^{-2} for 5min. B. deposit mass vs. deposition time in CXNa$_2$ and CNT suspension curve at 10 A m^{-2}. C,D. SEM images of deposited CXNa$_2$
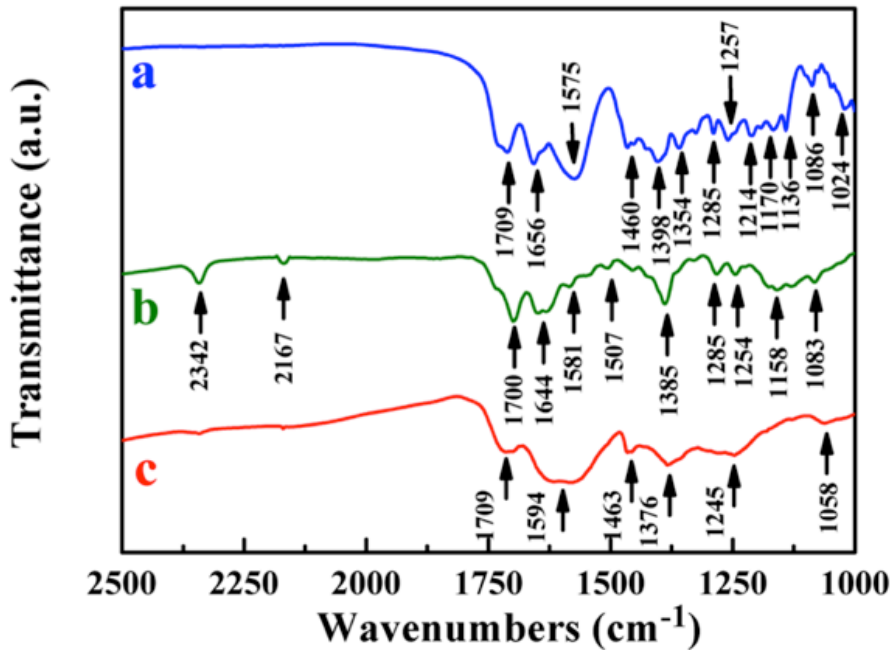
Fig 6-4 FTIR results (a) CXNa$_2$ powder, (b) deposited CXNa$_2$ and (c) deposited CNT with CXNa$_2$

The suggested deposition mechanism was confirmed by FTIR. The salified COONa groups of $CXNa_2$ contributed [71] to a broad adsorption peak (Fig 6-4 a) at 1575 cm^{-1}, However, it was not observed in the spectrum (Fig 6-4 b) of the film material, where carboxylic (COOH) groups were protonated. The absorptions [72] due to C═O stretching at 1700 and 1709 cm^{-1} and C─C stretching at 1656 and 1644 cm^{-1} were also observed. The absorptions at 1385 cm^{-1} resulted [73] from C─O stretching.

The deposition experiments, performed with 0.5-3 g L^{-1} $GANH_3$ and TDNa solutions did not result in film formation. It is suggested that electrostatic repulsion of the GA^- and TD^- species and relatively high solubility of the protonated molecules prevented film formation.

As shown in Fig 6-5, for B and C, there are still some pure PPy particle agglomerations, but in D, it was the ideal morphology of composite material with a thin layer of PPy wrapping around MWCNTs, which makes the materials more electric conductive and porous, which gives the best electrochemical performances.
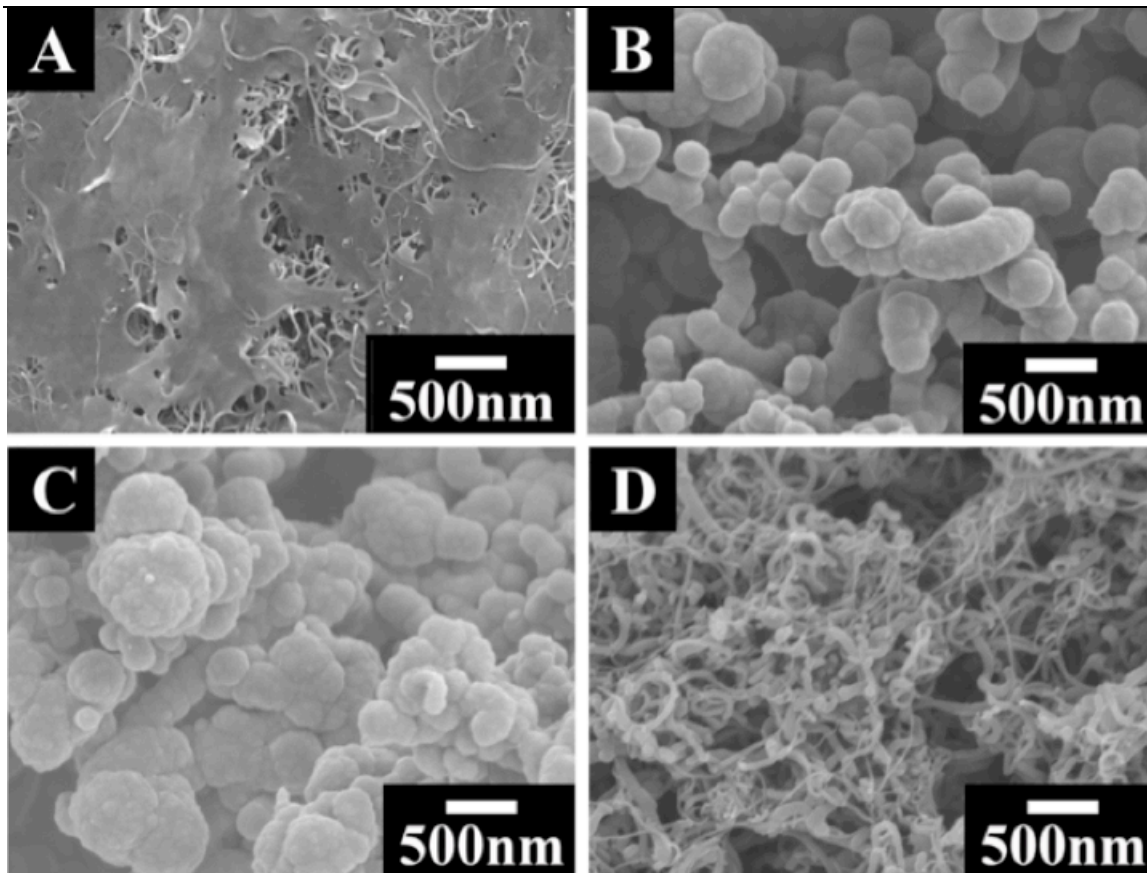
Fig 6-5 SEM images of deposited samples at current density of 10 A m^{-2} for 5 min (a) deposit of 1 g L^{-1} CXNa$_2$ and 1 g L^{-1} CNT suspension (for comparison), (b) deposit of 0.5 g L^{-1} CXNa$_2$, 1 g L^{-1} CNT, 0.2mol L^{-1} Py and 0.01mol L^{-1} Tiron mixture, (c) deposit of 0.5 g L^{-1} GANH$_3$, 1g L^{-1} CNT, 0.2mol L^{-1} Py and 0.01mol L^{-1} Tiron mixture, (d) deposit of 0.5 g L^{-1} TDNa, 1g L^{-1} CNT, 0.2mol L^{-1} Py and 0.01mol L^{-1} Tiron mixture.

6.1.2 CVs and Capacitance

Electrochemically deposited samples were investigated by cyclic voltammetry tests and the results are shown in the following Figure 6-6, from which it can be clearly seen that sample with TDNa as dispersing agent had better shaped CV with a larger integrated area, a higher responding current to the changing potential and it led to higher capacitance. Lower capacitances of samples using the other two dispersants may be caused by PPy particle agglomerates that leads to poor access of electrolyte into electrode materials and

bad attachments between PPy and MWCNTs causing poor electric conductivity and dispersing agents self deposition.
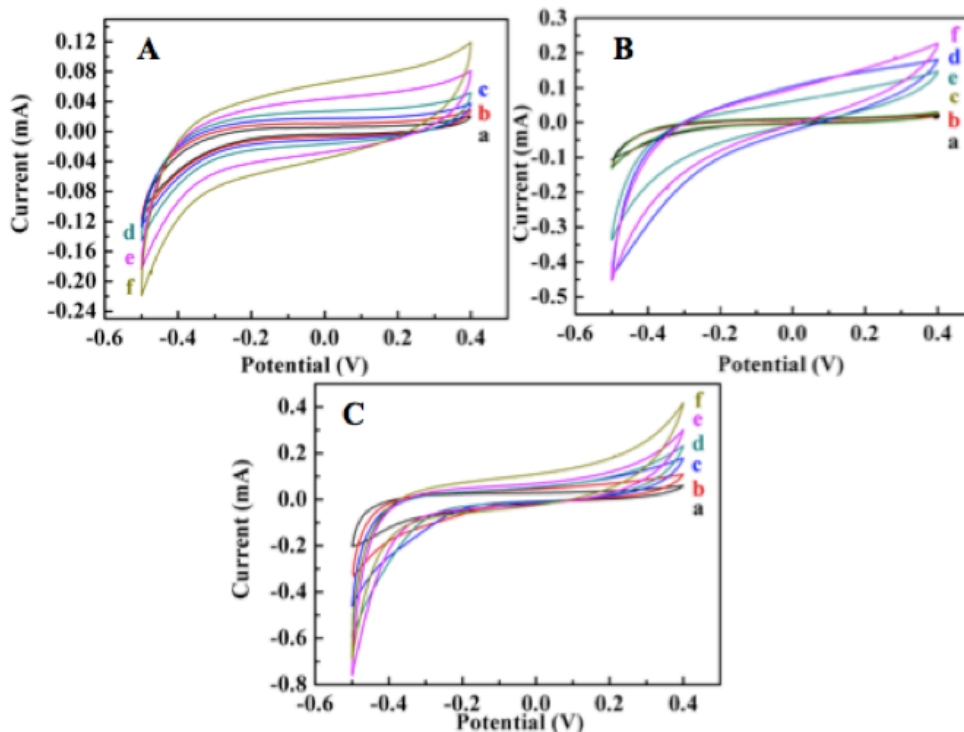
Fig 6-6 CV curves of deposited samples. A. $CXNa_2$ as dispersant, B. $GANH_3$ as dispersant and C. TDNa as dispersant, where a to f represent curves at scan rates of 2, 5, 10, 20, 50 and 100 mV s^{-1}.

Table 6-1 lists capacitances of samples using $CXNa_2$, $GANH_3$ and TDNa. Active material loadings for electrochemically deposited samples were 104.6, 104.8 and 111.1 μg cm^{-2}, respectively and it can be obtained by controlling deposition time under fixed current density (1 mA cm^{-2}) and solution concentrations. Capacitances can be calculated using Equation 5-1. Thin film samples have relatively poor retention and during charging-discharging process, film swelling and shrinkage may cause reduced adhesion,

even film peeling off substrate and it can be concluded from capacitance results in the

following table that the ratio of capacitance at 100 mV s^{-1} to capacitance at 2 mV s^{-1} is

relatively low.

Table 6-1 Capacitance results corresponding to Fig 6-6

Dispersant	Mass loading	Capacitance (F g^{-1})					
		2 mV s^{-1}	5 mV s^{-1}	10 mV s^{-1}	20 mV s^{-1}	50 mV s^{-1}	100 mV s^{-1}
CXNa$_2$	104.6 μg cm^{-2}	27.86	18.09	13.41	9.86	6.19	4.32
GANH$_3$	104.8 μg cm^{-2}	31.89	13.58	8.17	7.49	6.99	5.02
TDNa	111.1 μg cm^{-2}	133.34	75.21	43.36	21.13	9.30	5.79

Since deposited samples have poor performances and high active material mass loading is

essential for practical applications, chemical synthesis of PPy and PPy/MWCNT

composite materials was then conducted using the same three dispersants and the dopant.

Powders were synthesized with molar ratio of Py to dopant 10:1 and mass ratio of PPy to

MWCNT 7:3 and the CVs are shown in Fig 6-7, where curve a to e represent CV results

at 2, 5, 10, 20, 50 and 100 mV s^{-1}, respectively.

CV curves of chemically synthesized bulk materials deviated greatly from ideal box

shape with mass loading controlled around 29-33 mg cm^{-2}, especially under high scan

rates, but had a much larger integrated area and better retention than deposited samples.

Among these three dispersants, TDNa still gave the best performance and capacitance

results of samples with CXNa$_2$ and GANH$_3$ are presented in Fig 6-8. The highest specific

capacitance (SC) was nearly 65 F g^{-1} and the capacitance retentions of powders

containing $CXNa_2$ and $GANH_3$ were only around 23%, which can be calculated from

corresponding data at 2 mV s^{-1} and 100 mV s^{-1}.
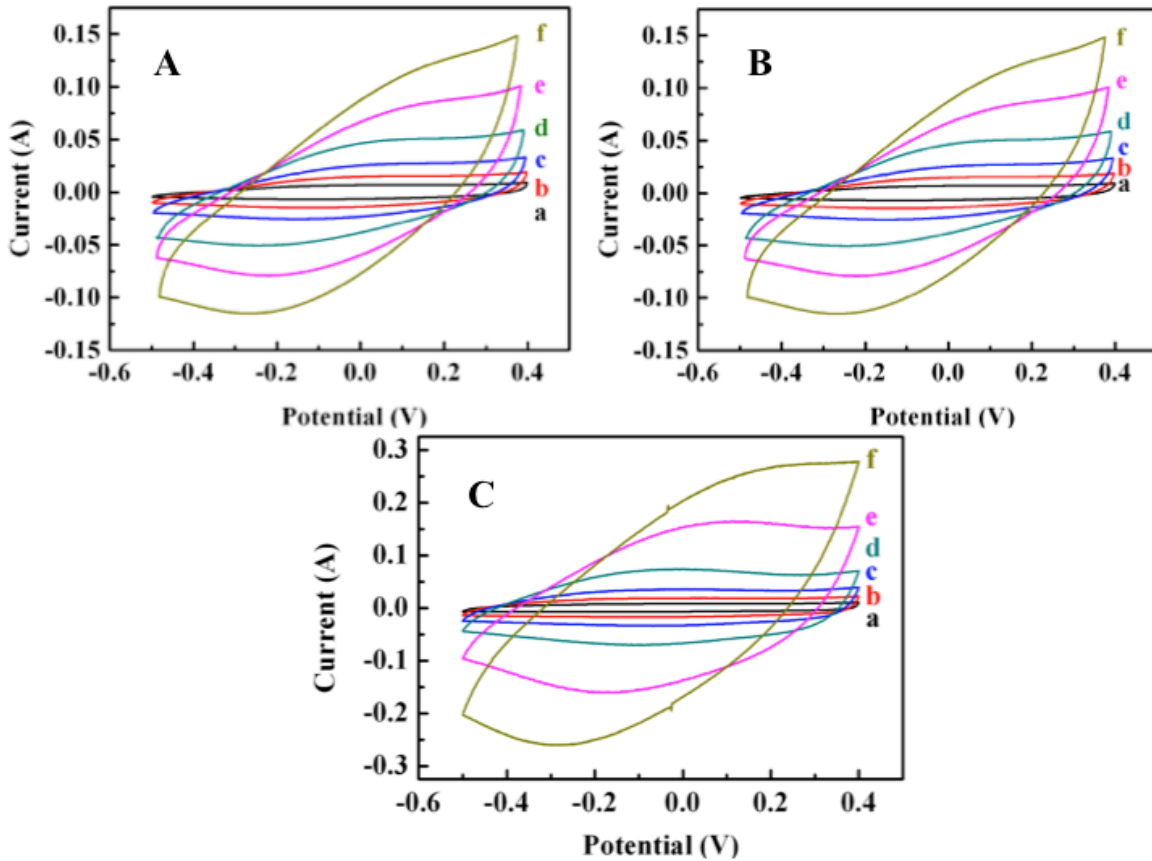
Fig 6-7 CV curves of chemically synthesized bulk materials. A. $CXNa_2$ as dispersant, B. $GANH_3$ as dispersant and C. TDNa as dispersant, where a to f represent curves at scan rates of 2, 5, 10, 20, 50 and 100 mV s^{-1}.
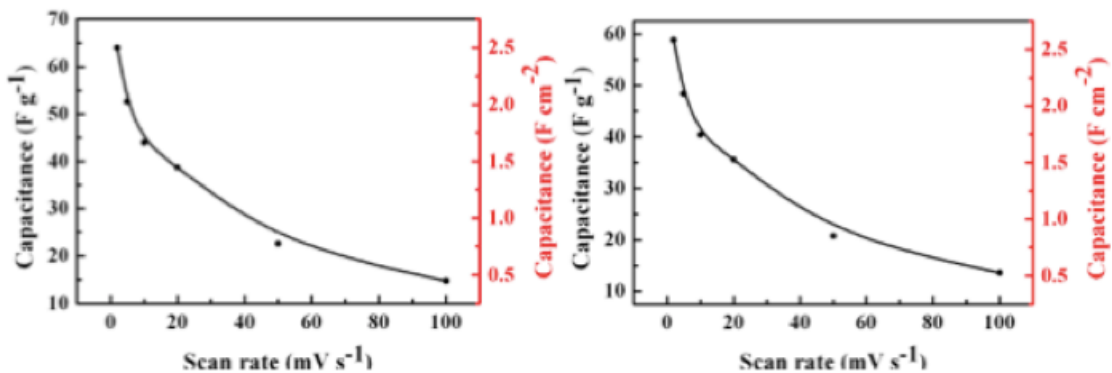
Fig 6-8 Capacitance results of bulk samples using CXNa$_2$ (right) and GANH$_3$ (left)

On the contrary, samples with TDNa as dispersant for MWCNT showed much more improved properties. Fig 6-9 is a comparison between chemically synthesized bulk materials and electrochemically deposited samples using TDNa as dispersing agent, where bulk material sample has a much better retention and with higher mass loading. Capacitive properties were compromised under low scan rates. The SC reached around 110 F g^{-1} (3.21 F cm^{-2}) at scan rate of 2 mV s^{-1} with capacitance retention reaching 42%. And compared to the two samples in Figure 6-8, PPy/MWCNT powders with TDNa have much higher capacitance and better cycling stability.
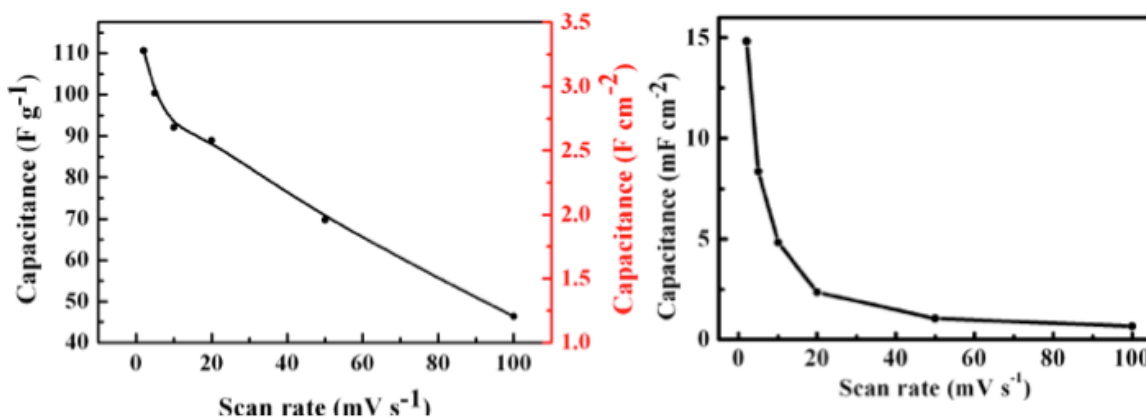
Fig 6-9 Capacitance results of bulk (left) and deposited (right) samples with TDNa as dispersant

6.1.3 Summary

In this research, CXNa$_2$, GANH$_3$ and TDNa were utilized as dispersing agents for

MWCNTs in electrochemical and chemical polymerization of PPy/MWCNT composites and with all of these dispersants, suspensions were stable for months. $CXNa_2$ could deposit itself and it led to reduced capacitance due to less access of electrolyte towards active materials. With TDNa, good dispersion of MWCNT can be obtained, which makes the electrode materials more stable and porous with a thin layer of PPy coating on MWCNTs. Better retention and higher capacitance were achieved by using chemically synthesized bulk materials. Among the three dispersants, TDNa gave the best performances and the capacitance reached 110 F g^{-1} (3.21 F cm^{-2}). Since TDNa performances well electrochemically, it will be continuously utilized in later research for dispersion of MWCNT.

6.2 Chemical polymerization of PPy/MWCNT doped with multifunctional dopants

Multifunctional dopants can act as dispersing agents for MWCNT and dopant for PPy at the same time and the selection of effective multifunctional dopants are beneficial for doping and synthesis of PPy/MWCNT concerning cost, ease of processing and other factors. Using multifunctional dopants the total concentration of electrochemically inactive additives can be reduced. In this case higher capacitance of the composite materials can be expected. In this research, Eriochrome Cyanine R (ECR), 4-Amino-5-hydroxy-2, 7-naphthalenedisulfonic acid monosodium salt hydrate (AHN)

and 3-Hydroxy-4-nitroso-2, 7-naphthalenedisulfonic acid disodium salt (HNN) were investigated and the chemical structures are shown in Figure 4-2 with multiple benzene rings and charged groups, which can connect with MWCNT through π-π interaction and disperse MWCNT through electrostatic repulsions.

6.2.1 Morphology Characterization

Multifunctional dopants can function as dispersants for MWCNT and promote PPy deposition on MWCNT during chemical synthesis. Fig.6-10 shows PPy-MWCNT composite, prepared using ECR. PPy powders with ECR, AHN and HNN were prepared by steps shown in Figure 5-1 (a). Multifunctional dopants can function as dispersing agents for MWCNT and the SEM image (Fig 6-10) shows that the MWCNTs are well dispersed and coated with a thin layer of PPy with the presence of ECR. And the PPy particles were not observed in the SEM images. However, compared to deposited PPy and PPy powders prepared with Tiron, particle size of polymer was reduced to nearly 100 nm.
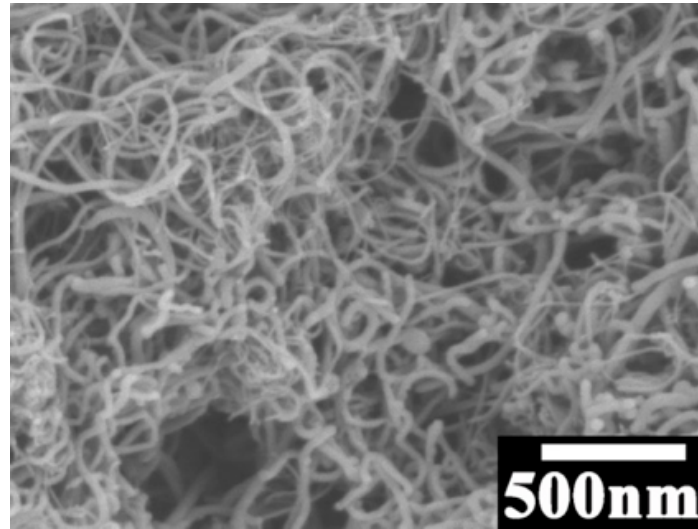
Fig 6-10 SEM image of PPy-MWCNT composite powder, prepared using ECR as a dopant for PPy and dispersant for MWCNT
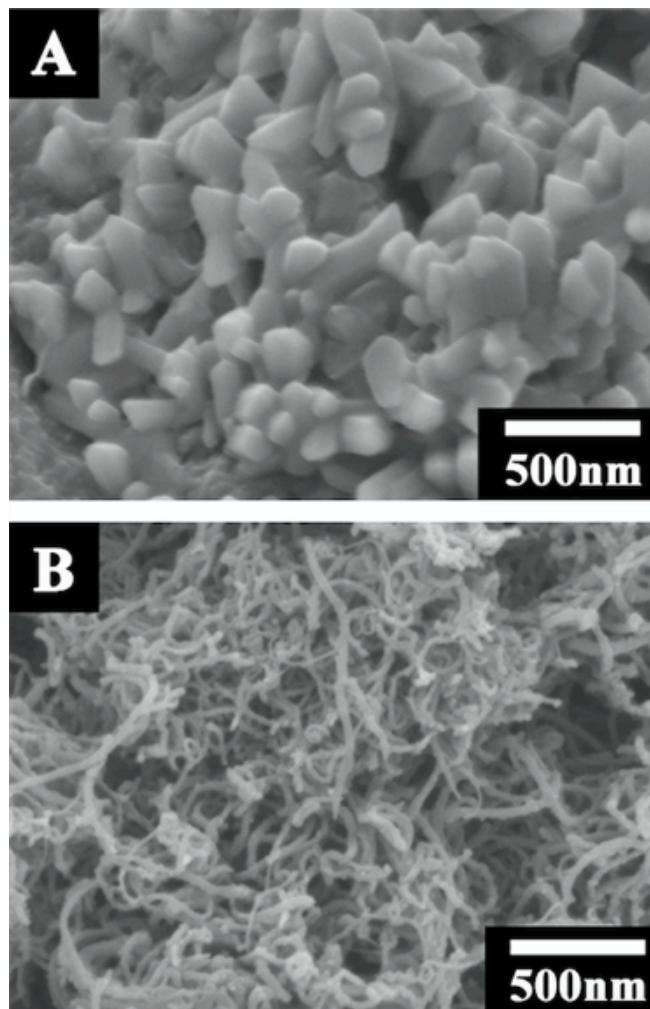
Fig 6-11 Comparison between pure PPy prepared using AHN (A) and MWCNT coated

with PPy using AHN (B)
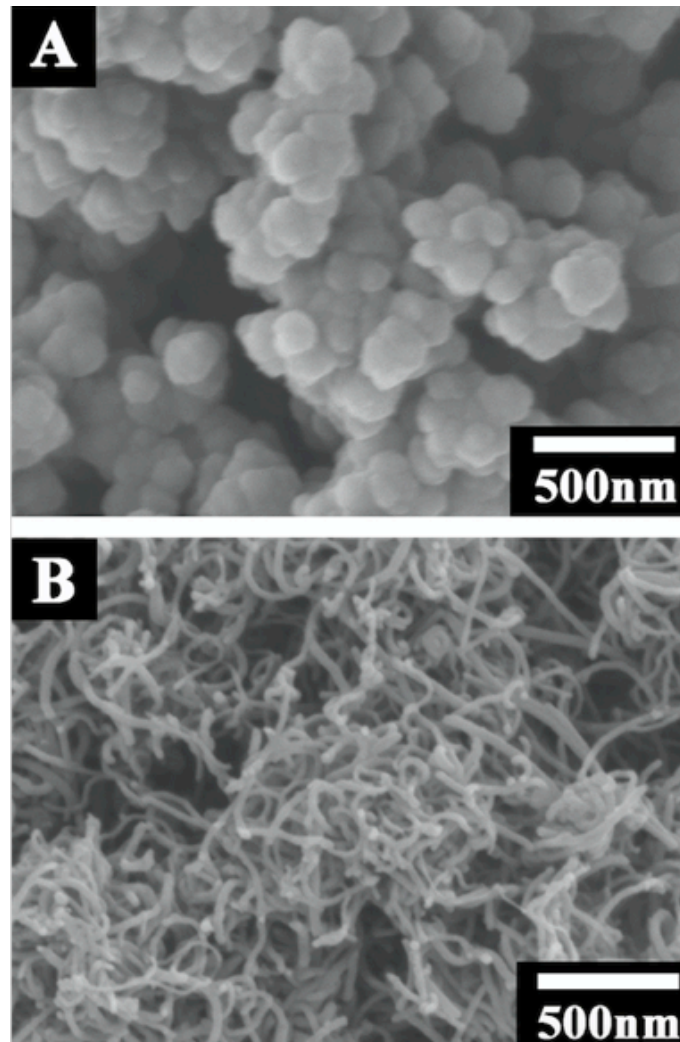
Fig 6-12 Comparison between pure PPy with HNN (A) and MWCNT coated with PPy with HNN (B)

Fig 6-11 and Fig 6-12 are SEM morphology comparisons between pure PPy particle and composite materials of PPy-MWCNT, prepared using AHN and HNN, respectively. AHN and HNN were used as dopants for PPy and dispersants for MWCNT. The SEM images of the pure PPy show relatively large particles, which have a typical size of 10-200 nm. The particles formed larger agglomerates. Such large particles were not

observed in the SEM images of PPy-MWCNT composite powders. The SEM images of

such powders show a fibrous morphology, indicating that PPy was deposited on

MWCNT during synthesis. The results indicated that the dispersants, adsorbed on

MWCNT and promoted PPy film formation on the MWCNT surface, resulting in the

formation of PPy coated MWCNT. The PPy coated MWCNT offer benefits for

supercapacitor applications, because in this case electrical contact of PPy and CNT is

improved. Moreover, relatively large PPy particles and agglomerates limit electrolyte

access to the PPy bulk material. This problem was avoided by the formation of thin PPy

layers on the MWCNT surface and preventing the formation of large PPy particles and

their agglomerates.

6.2.2 CVs and Capacitance

ECR showed better dispersion of MWCNT, compared to AHN and HNN. The improved

dispersion can result from a different chemical structure, which can be beneficial for ECR

adsorption on MWCNT. It is important to note, that ECR, AHN and HNN have nearly

the same charge to mass ratio. However, larger size and larger charge to mass ratio of

ECR can be beneficial for electrostatic dispersion of MWCNT. Moreover, polycharged

dopants, such as ECR can create links between PPy chains, promoting charge transfer.

The PPy/MWCNT composites, prepared using ECR showed excellent electrochemical

performance, as it was indicated by the ideally box-shaped CV curves (Fig 6-13) and

high capacitance that reaches more than 100 F g^{-1}. The powder was synthesized with a

molar ratio of Py to ECR 10 to 1 and molar ratio of Py to oxidant APS 1 to 3. And

MWCNT takes up 30% of the total weight of composite material. The current increased

with increasing scan rate, indicating good capacitive response and good capacitance

retention at high charge-discharge rates.
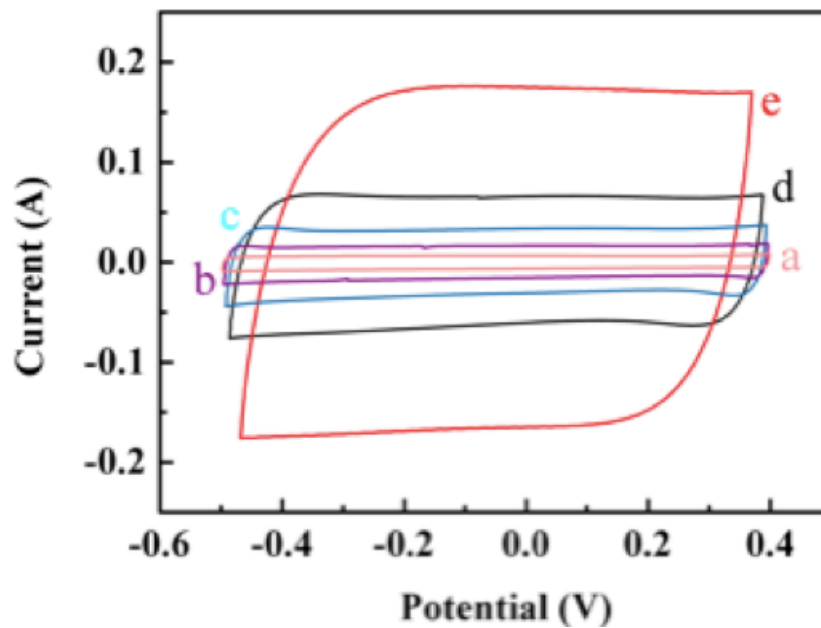
Fig 6-13 CV curves of bulk sample with ECR, where a to e represent curves at scan rates of 2, 5, 10, 20 and 50 mV s^{-1} (mass loading 31.61 mg cm^{-2})
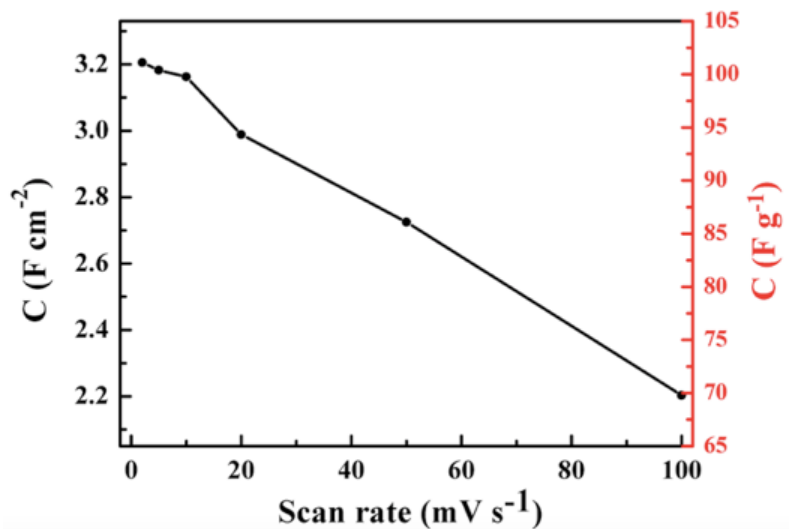
Fig 6-14 Capacitance results of bulk sample with ECR (mass loading 31.61 mg cm^{-2})

As can be clearly seen in Fig 6-14, the capacitance of PPy-MWCNT electrodes, prepared using ECR reached 3.2 F cm^{-2} and around 101 F g^{-1} and the sample showed really good retention with nearly 70 F g^{-1} at the scan rate of 100 mV s^{-1} (almost 70% of capacitance retention). The remarkably high capacitance and excellent capacitance retention at high charge-discharge rates are important for practical applications in high power supercapacitors. However, powders with AHN and HNN did not perform as well as powders with ECR.
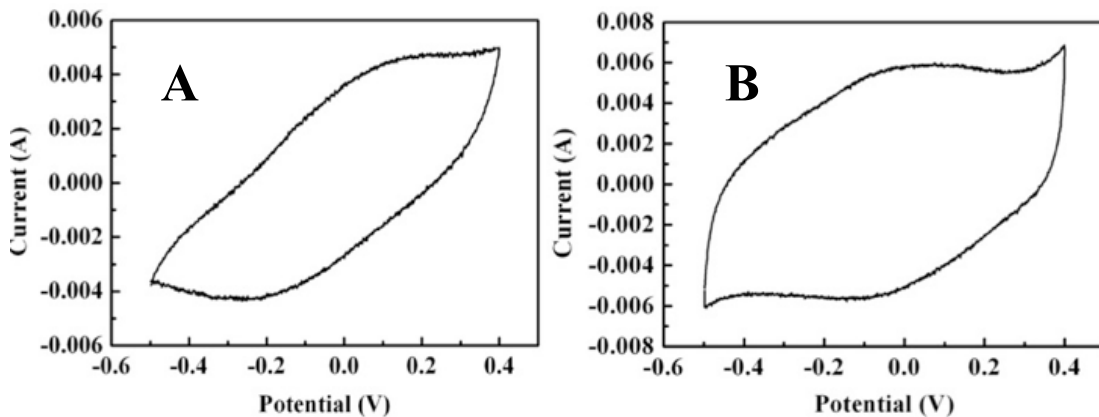
Fig 6-15 CV curves at 2 mV s^{-1} of bulk sample with AHN, where A is pure PPy and B is PPy/MWCNT composite material.
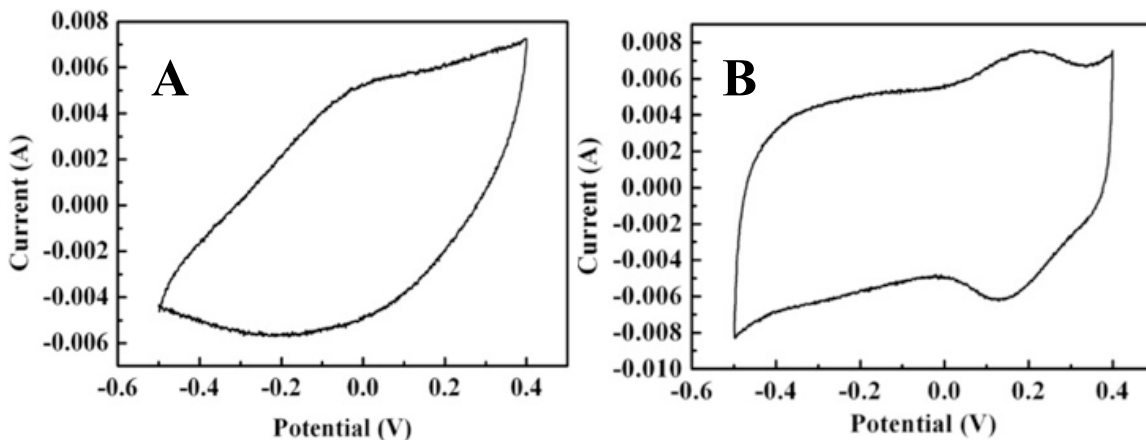
Fig 6-16 CV curves at 2 mV s^{-1} of bulk sample with HNN, where A is pure PPy and B is PPy/MWCNT composite material.

Figure 6-15 and Figure 6-16 are CVs of chemically synthesized bulk samples containing AHN and HNN at scan rate of 2 mV s^{-1}, from which it is clearly presented that with the addition of MWCNT, the CV curves are closer to box shape with higher current, faster ions adsorption/desorption kinetics responding to changing current and larger integrated area, meaning that samples with MWCNTs can store more charges than pure PPy.

However, the capacitive performance of samples with AHN and HNN were not as good as the ones with ECR. The materials, prepared using AHN and HNN showed different CV shapes, which deviated significantly from ideal box shape. The presence of peaks in Figure 6-16 may be caused by irreversible redox reactions. After powder drying out, when being prepared for fabrication of electrode, the powders can not be uniformly dispersed in ethanol, which leads to agglomeration presence on the electrode. And as a result, with larger mass loading of materials, the surface of current collector was covered, blocking the impregnation of the bulk of the current collector. From the Table 6-2 of capacitance data, it can be concluded that HNN allowed for better electrochemical performance than AHN. The PPy-MWCNT composite materials showed larger capacitances, compared to the capacitances of pure PPy materials, prepared using the same dopants-dispersants. It is important to note, that in this investigation relatively large mass loadings were used, which are important for practical applications. It is known from the literature that gravimetric capacitance decreased drastically with increasing active mass loading due to poor electrolyte access to the bulk material. However, the composites, prepared in this work, retained relatively large gravimetric capacitance at relatively high active mass loadings. As a result, remarkably high areal capacitances were achieved. It is in this regard, that typical mass loading in the literature were about 0.1-2 mg cm^{-2}, which allowed for a relatively low active mass to current collector mass ratio

(M_r) below 2-3%. In contrast, in our investigation, M_r was always above 50%. The high

M_r is of critical importance for the manufacturing of efficient supercapacitor devices.

Table 6-2 Capacitance results of bulk samples with AHN and HNN

Composition	Mass loading	Capacitance at 2 mV s^{-1}	
AHN PPy	33.7 mg	32.18 F g^{-1}	1.08 F cm^{-2}
AHN PPy with MWCNT	36.3 mg	57.17 F g^{-1}	2.08 F cm^{-2}
HNN PPy	38.7 mg	44.30 F g^{-1}	1.71 F cm^{-2}
HNN PPy with MWCNT	33.9 mg	79.89 F g^{-1}	2.71 F cm^{-2}

6.2.3 Impedance

Impedance data was collected in a wide frequency range and presented in a Nyquist plot

in Figure 6-17. The Nyquist plot showed relatively low resistance Z'=R, the slop of the

curve is close to 90º. Such plot indicates good capacitive behavior. The slope of

impedance curve in low frequency area represents electrolyte diffusion into porous active

material and protons diffusion into host material, which can be described by Warburg

impedance (W) [74, 75]. The larger the slope of the curve in low frequency area, the

lower the diffusion resistance. As a result, ideal impedance plot for supercapacitors

should be straight line parallel to the imaginary impedance Z'' axis. In high frequency

area, the intersection of the curve at real impedance Z' axis is the resistance of the system.

The resistance of bulk sample can be read directly from the following impedance plot and

the resistance of sample with ECR is as low as 0.5 Ohm.
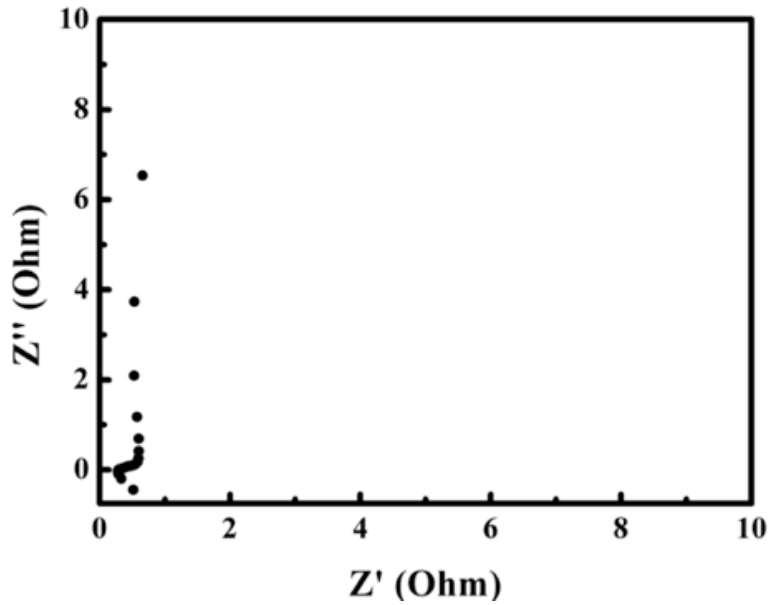
Fig 6-17 Impedance plot of PPy-MWCNT composite, prepared using ECR (mass loading
31.61 mg)
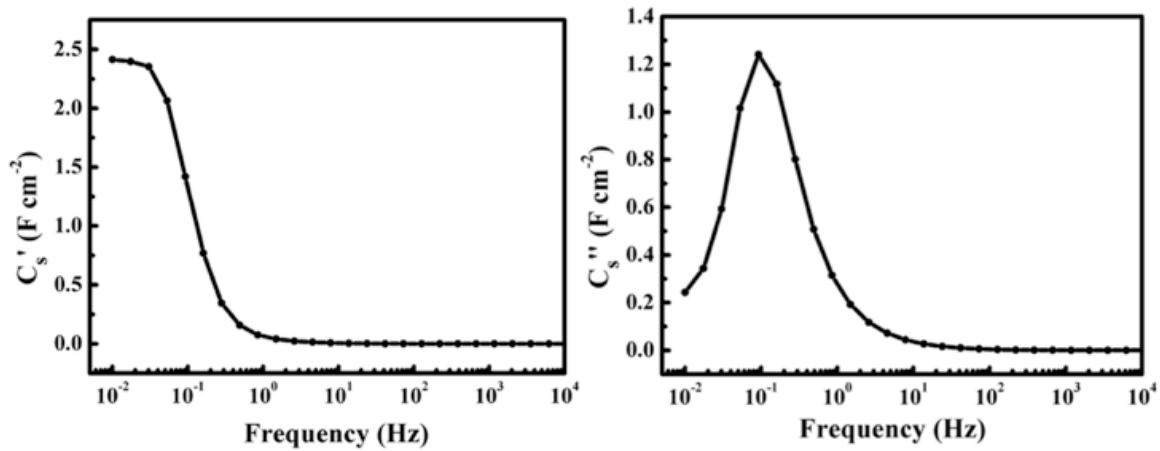
Fig 6-18 Real (left) and imaginary (right) capacitance calculated from impedance plot
(mass loading 31.61 mg)

Impedance data provides an alternative way to analyze capacitance of samples. Two parts of complex form of capacitance (C_S^*) are real capacitance (C_S') and imaginary capacitance (C_S''). As the frequency increases, real capacitances present continuous reduction and eventually remain constant, while imaginary capacitance increases to a peak and then decreases sharply and the peak frequency corresponds to the frequency where slope of real capacitance reaches the most negative value. The decline of real capacitance may be due to the failure of ions diffusion with high external power frequency, which also explains the peak in the imaginary capacitance curve.

Fig.6-18 and 6-19 show Nyquist impedance plots for PPy-MWCNT electrodes and pure PPy electrodes, prepared using AHN and HNN. The electrodes, prepared without MWCNTs showed relatively high resistance. The slop of the plot deviated significantly from 90º. Such behavior resulted from poor electrolyte access to the bulk of PPy and low electronic conductivity. The addition of MWCNT resulted in improved capacitance behavior, as it was indicated by the increased slope of the graphs and reduced resistance. This behavior correlates with differences in morphology of materials, discussed above, and contribution of carbon nanotubes to the electronic conductivity.
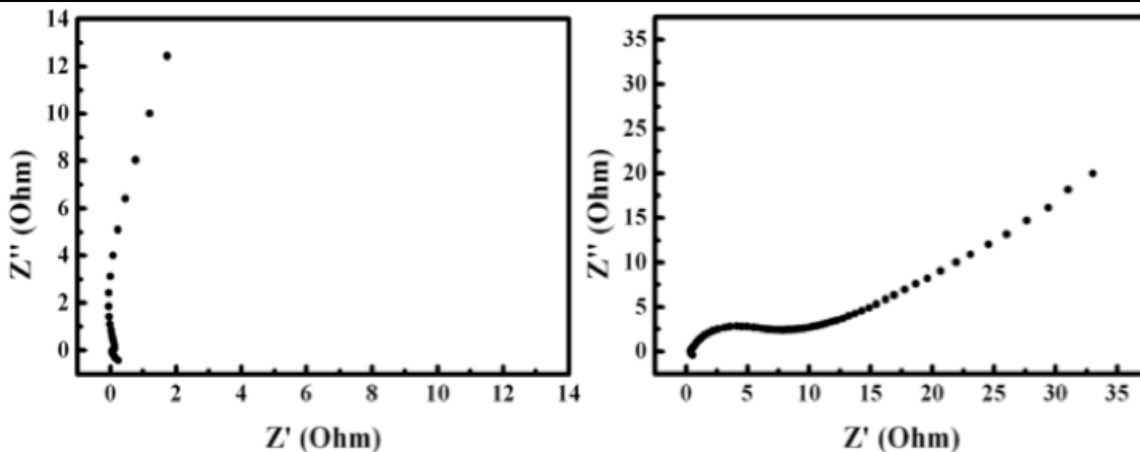
Fig 6-19 Nyquist impedance plots of PPy-MWCNT electrodes (left) and pure PPy electrodes (right) with AHN
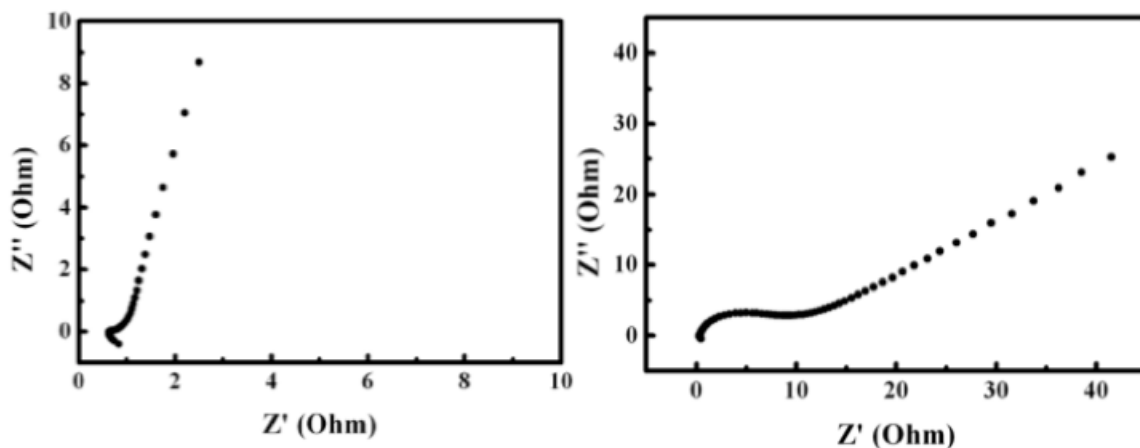
Fig 6-20 Nyquist impedance plots of PPy-MWCNT electrodes (left) and pure PPy electrodes (right) with HNN

Semicircles in high frequency area of impedance plot are related to double layer capacitance and charge transfer resistance, which can present charge transfer process taking place on the working electrode and electrolyte interface. There was nearly no semicircle observed in pictures on the left in Figure 6-19 and Figure 6-20, which indicates that with the addition of MWCNT, the charge transfer resistance was significantly reduced. When compared to ECR, with AHN and HNN, the electrode

performed poorly in low frequency area, and with HNN, the bulk resistance of the electrochemical system is slightly higher than samples with ECR and AHN.

6.2.4 Summary

With the addition of MWCNT, PPy polymer backbone was enhanced in terms of mechanical stability and electric conductivity. Using multifunctional dopants makes it easier to produce PPy/MWCNT powders due to the reduction of steps of synthesis and usage of chemicals. ECR is a promising multifunctional dopant. The powders synthesized with ECR have good capacitive behavior, as indicated by a high capacitance of 100 F g^{-1} (3.21 F cm^{-2}), high capacitance retention of around 70% of capacitance at low scan rate and low impedance around 0.5 Ohm with nearly vertical Nyquist plot of complex impedance parallel to Y-axis. However, AHN and HNN gave poorer performances, including less retention, lower capacitance, higher diffusion resistance and higher bulk resistance of electrochemical system. When compared with ECR, it indicates that multifunctional dopants possessing larger molecular size and multiple charged groups may promote the growth of porous polymer matrix and good dispersion of MWCNT. However, with modification of concentrations and molar ratios of multifunctional dopants to Py monomer, they still can serve as multifunctional dopants.

6.3 Chemical polymerization of PPy/MWCNT doped with Aromatic Dopants

Aromatic dopant molecules can modify PPy morphology and enhance conductivity. Anionic dopants with multiple charged groups will increase doping efficiency and may form interlink between polymer chains, which can improve interchain charge mobility. Tiron and FDS are dopants with aromatic ring and two negatively charged groups, whose chemical structures are shown in Fig 4-1. Since TDNa is so far the best dispersing agent for MWCNT, it was utilized in this part of research.

6.3.1 CVs and Capacitance

MWCNTs act as a reinforcement for polymer backbone, which enhances not only mechanical stability, but also electric conductivity and porosity. However, MWCNT has relatively low capacitance, and with high quantities of MWCNT, the capacitance of composite materials may be reduced. To synthesize PPy/MWCNT composites, the mass ratio between polymer and MWCNT has to be optimized. Another important parameter is the mass ratio of Py and dopant in the starting solution for chemical polymerization. Based on previous group work [3, 66], mass ratio of PPy to MWCNT 7 to 3 and 4 to 1 give better performance. A comparison experiment was conducted using Tiron as a dopant and TDNa as a dispersant. The CV results are shown in Fig 6-21 for electrodes with different MWCNT contents.
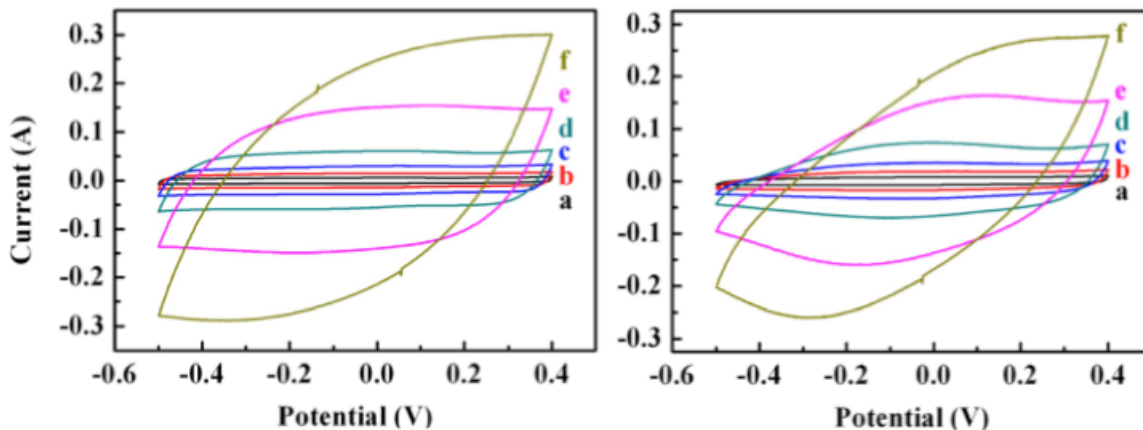
Fig 6-21 CV curves of PPy powder with 30 wt% of MWCNT (left) and PPy powder with 20 wt% of MWCNT (right), where a to f represent curves at scan rates of 2, 5, 10, 20, 50 and 100 mV s^{-1}.

The composite material with 30 wt% of MWCNT has larger CV curve areas, the shapes of the CVs were closer to the ideal box shape. Capacitance values, calculated from CV curves for PPy/MWCNT composite powders with 30 wt% and 20 wt% of MWCNT are listed in the Table 6-3, from which it can be clearly concluded that with 30 wt% of MWCNT, the capacitance retention of the electrode during test reached 58.7%, compared to the capacitance retention of 41.9% for the sample of 20 wt% of MWCNT calculated using corresponding capacitances at scan rates of 2 and 100 mV s^{-1}. However, with a higher percentage of MWCNT, the capacitance was slightly lower at 2 mV s^{-1}, which makes sense since MWCNT has relatively low capacitance.

Table 6-3 Capacitance of PPy powders with 30 wt% and 20 wt% of MWCNT

Scan rates (mV s^{-1})		2	5	10	20	50	100
Capacitance 30 wt% MWCNT (30.9 mg cm^{-2})	F g^{-1}	90.23	87.00	84.11	82.21	72.30	53.00
	F cm^{-2}	2.79	2.69	2.60	2.54	2.23	1.64
Capacitance 20 wt% MWCNT (29 mg cm^{-2})	F g^{-1}	110.6	100.4	92.07	88.96	69.71	46.36
	F cm^{-2}	3.21	2.91	2.67	2.58	2.02	1.34

To investigate influence of mass loading of active materials in current collector on final capacitance of electrode, a series of experiment were conducted using molar ratio of dopant Tiron to Py monomer 10 to 1 at scan rate of 2 mV s^{-1} and the relationship between mass loading and capacitance is shown in Fig 6-22, which indicate that with increasing mass of active materials, the capacitance decreases. It is believed that the higher the mass loading, the thicker powders pasted on porous nickel foam and the more difficult for electrolyte to gain access to interior material. Therefore, the capacitance is not as high as expected. And it also illustrates that electrodes of similar mass loadings must be compared in terms of capacitive properties.
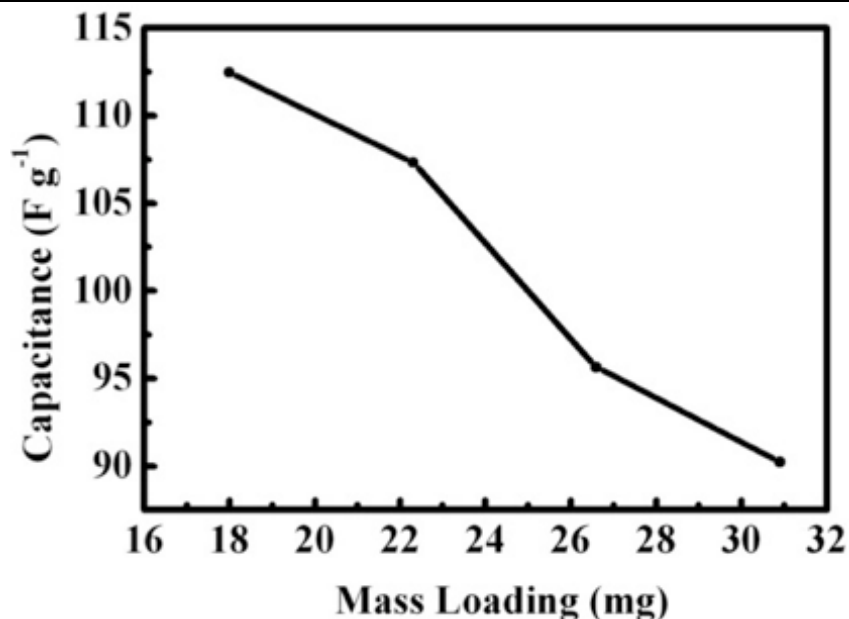
Fig 6-22 Gravimetric capacitance vs active mass loading for PPy electrodes with molar ratio of Tiron to Py 1 to 10 at a scan rate 2 mV s^{-1}

In order to find the optimum amount of dopant, previous work used the Py monomer to dopant molecule molar ratio of 10 to 1. A series of experiment was conducted for comparison and optimization of utilization of anionic dopant. The experiments were designed using different molar ratio between Py monomer and dopant molecule, which were 10 to 1, 5 to 1 and 3 to 1, respectively. Since mass loading has an influence on capacitance results, the masses of active materials in current collector corresponding to each molar ratio were controlled at a similar level, which can be listed as 30.9, 28.8 and 29.3 mg cm^{-2}, respectively.
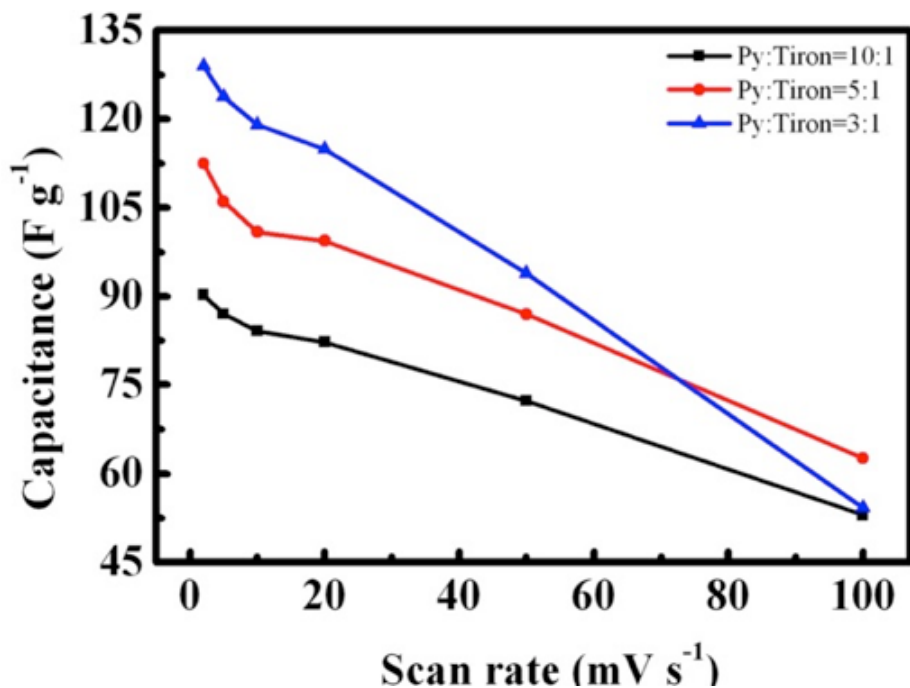
Fig 6-23 Comparison of capacitance between different compositions

Fig 6-23 clearly demonstrates that raising the amount of dopant can lead to improved capacitive properties and the optimal molar ratio between Py monomer and dopant is 3 to 1 and the powders perform better at low scan rates.

FDS has similar chemical structure to Tiron without two –OH groups and it was expected to function like Tiron. However, the usage of FDS enables extremely small particle size and PPy powders kept going through filter membrane with pore sizes of 1 μm and 0.45 μm. As a result, a great deal of effort has been invested in developing method to filter suspension and obtain powders with FDS. Pure PPy powders were left on the membrane in a small quantity, but when fabricated into an electrode, the powders kept peeling off,

even with 5 wt% of binder and the electrode cannot be tested. And for composite material, the binding between PPy and MWCNT was poor and there were still a lot of PPy particles not combined with MWCNT. To solve this, Safranin O (SAF) (Fig 6-24) was used as a co-dispersant to try to synthesize composite materials [76]. This time, powders can be filtrated, but the capacitances were relatively low compared to composites, prepared using Tiron.
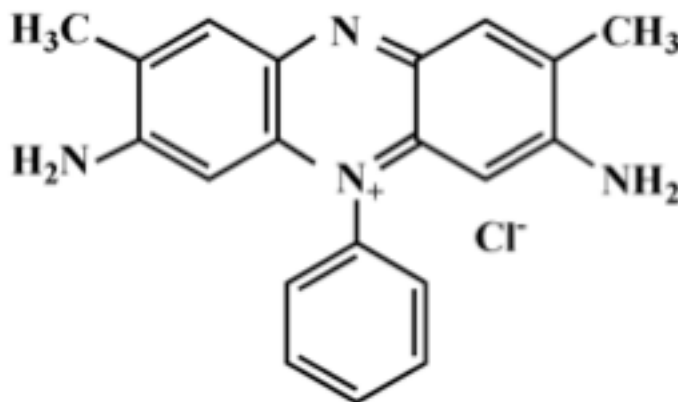
Fig 6-24 Chemical structure of SAF

Fig 6-25 shows capacitive behavior of PPy-MWCNT composites with PPy/MWCNT mass ratio of 17:3. The obtained CVs were tilted and their shapes at different scan rates deviated significantly from the ideal box shapes. The tilted CVs indicated significant resistance of the electrodes. The gravimetric capacitance was relatively low at 2 mV s^{-1} and decreased significantly with increasing scan rate. Fig.6-26 shows capacitive behavior of electrodes with lower MWCNT content. The CVs also deviated from ideal capacitive

behavior. The reduction in the MWCNT content resulted in reduced capacitance, especially at high scan rate.
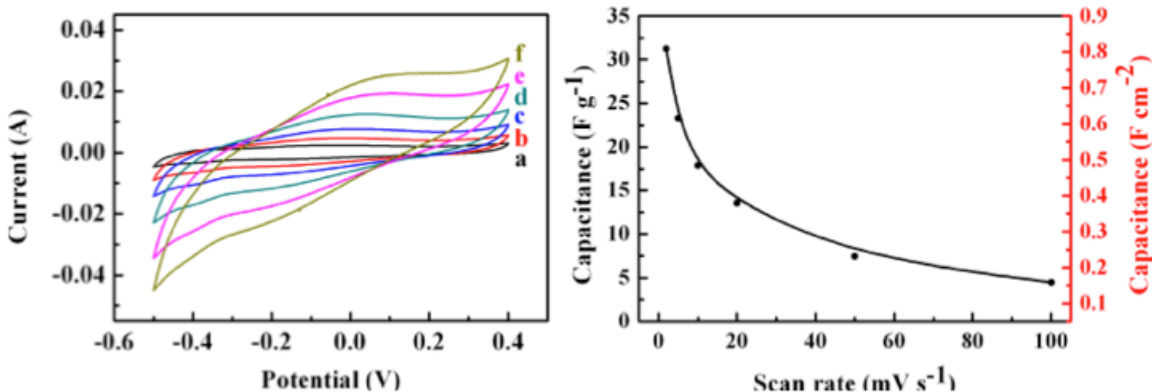
Fig 6-25 CV curves (left) and capacitance results (right) of FDS doped PPy/MWCNT mass ratio 17:3, where a to f represent curves at scan rates of 2, 5, 10, 20, 50 and 100 mV s^{-1} (mass loading of 26 mg).
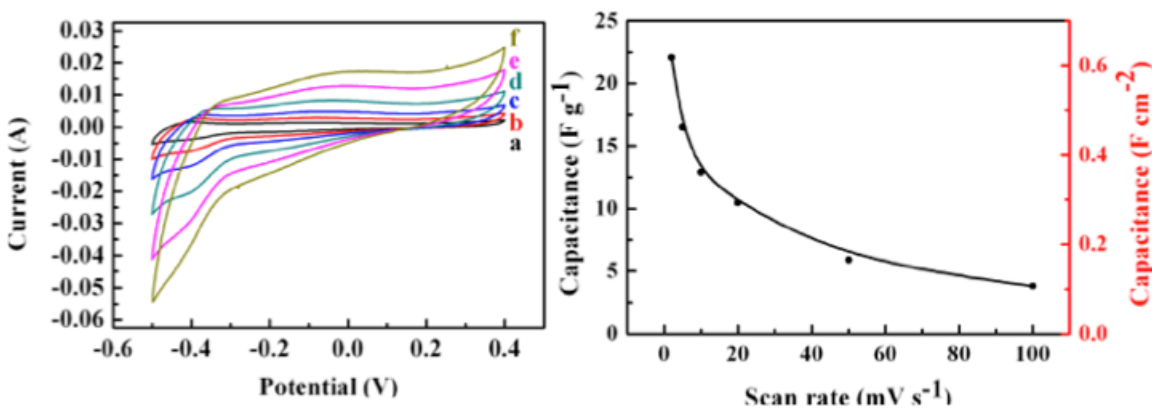
Fig 6-26 CV curves (left) and capacitance results (right) of FDS doped PPy/MWCNT mass ratio 4:1, where a to f represent curves at scan rates of 2, 5, 10, 20, 50 and 100 mV s^{-1} (mass loading of 28 mg).

New Fuchsin (NF) with $-NH_2$ groups was taken into consideration to help PPy

precipitate so that it will not go through filter membrane. Those $-NH_2$ may react with FDS and form precipitation. The strategy involved the use of NF as a dispersant for MWCNT and Schiff base reaction of FDS and NF, involving aldehyde groups of FDS and amino groups of NF. However, no improvement was achieved in the capacitive behavior of the composite PPy-MWCNT electrodes.

6.3.2 Summary

When synthesize PPy/MWCNT composite materials, the optimal PPy to MWCNT mass ratio was 7 to 3 with better retention reaching 58.7% and good capacitance results especially at higher scan rates. And mass loading of active materials also has an influence on final capacitance. Thus only electrodes with similar mass loading levels can be compared. Also the ideal molar ratio of Py monomer to dopant was finalized to 3 to 1 after a series of comparison experiments comparing three samples with similar mass loadings and the capacitance was improved by nearly 43% at scan rate of 2 mV s^{-1} from 90.23 F g^{-1} to 129.01 F g^{-1}. FDS was a promising chemical that could enable to achieve relatively small size of PPy particle, but unfortunately, PPy kept going through filter membrane, which makes it impossible to fabricate electrode for continuing testings. SAF and NF were used to try to help connect with MWCNTs and precipitate PPy, but did not show any improvement.

7 Conclusions

The electrochemical and chemical synthesis of PPy and PPy/MWCNT composite with different dopants, such as ECR, AHN, HNN, Tiron and FDS, and three dispersing agents, including $CXNa_2$, $GANH_3$ and TDNa, were studied in this research. Morphology analysis and electrochemical tests, including cyclic voltammetry and impedance were carried out for characterization in terms of capacitive properties.

The results showed that $CXNa_2$, $GANH_3$ and TDNa were good dispersing agents for MWCNT with which suspensions can be stable for months. However $CXNa_2$ could deposit itself that would lead to decreased capacitance due to less access of electrolyte towards active materials. Among these three dispersants, TDNa was the best and the suspension was stable up to 12 months. With TDNa, good dispersion of MWCNT can be obtained, which makes the electrode materials more stable and porous with a thin layer of PPy coating on MWCNTs. Better retention and higher capacitance were achieved by using chemically synthesized bulk materials. Among the three dispersants, TDNa gave the best performances, reaching 110 F g^{-1} (3.21 F cm^{-2}) with TDNa. Since composites, prepared using TDNa as a dispersant, showed enhanced electrochemical performance, it will be continuously utilized in later research for dispersion of MWCNT.

With the addition of MWCNT, the PPy polymer backbone was enhanced in terms of mechanical stability and electric conductivity. Multifunctional dopants enable simpler synthesis process of PPy-MWCNT composite materials due to reduction of steps of synthesis and usage of chemicals. ECR is a promising multifunctional dopant and powders synthesized with ECR have good capacitive behaviors achieving a capacitance of 100 F g^{-1} (3.21 F cm^{-2}), high capacitance retention of around 70% of capacitance at low scan rate and low impedance around 0.5 Ohm with nearly vertical Nyquist plot parallel to Y-axis in high frequency area. However, AHN and HNN gave poorer performances, including less retention, lower capacitance, higher diffusion resistance and higher bulk resistance of electrochemical system, which indicates that multifunctional dopants possessing larger molecular size and multiple charged groups may promote the growth of porous polymer matrix and good dispersion of MWCNT.

The results indicated that anionic dopants had great influence on microstructure and electrochemical properties. This research strongly support that dopants with multiple charged groups, high charge to mass ratio and large molecular size can promote capacitive behaviors for ES in a voltage window of -0.5~+0.4 V vs. SCE at low scan rate. Tiron with two –OH groups gave better performance. For composite materials, the optimal mass ratio was 7 to 3 with better retention reaching 58.7% and good capacitance results especially at high scan rates. Mass loading of active materials also has an

influence on final capacitance so that electrodes with similar mass loadings must be compared. Also the ideal molar ratio of Py monomer to dopant was finalized to 3 to 1 after a series of experiments comparing three samples with similar mass loading levels and capacitance was improved by nearly 43% at scan rate of 2 mV s^{-1} from 90.23 F g^{-1} to 129.01 F g^{-1}. FDS was a promising chemical that could enable to achieve relatively small size of PPy particle, but unfortunately, PPy kept going through filter membrane, which makes it impossible to fabricate electrode for continuing testings. SAF and NF were tried to help connect with MWCNTs and precipitate PPy, but did not show any improvement.

Chemical polymerization and current collector nickel foam with 95% of porosity allowed high mass loading up to 40 mg cm^{-2}, which was beneficial for practical use of electrochemical supercapacitors compared to deposited thin film samples.

8 Future Work

To develop advanced materials (CPs) for ES, monomer, dopants and dispersing agents should be taken into consideration at the same time. PPy is a promising conducting polymer with higher electric conductivity and theoretical capacitance compared to other CPs. However, fabrication of copolymers and further research about Py derivatives with functional groups are also worth investigation for application of CPs in electrochemical

supercapacitors field.

MWCNT reinforced PPy performs much better than pure PPy and investigations on developing optimum ratio and composition should be continued.

Anionic dopants for Py should be multiple charged with high charge-mass ratio and also have aromatic structure with high molecular size. Selection of dopants can be based on these requirements. FDS is a promising dopant and fabrication related problem should be addressed.

REFERENCES

[1] A. Burke, "Ultracapacitors: why, how, and where is the technology," *J. Power Sources*, vol. 91, no. 1, pp. 37–50, 2000.

[2] G. Wang, L. Zhang, and J. Zhang, "A review of electrode materials for electrochemical supercapacitors," *Chem. Soc. Rev.*, vol. 41, no. 2, pp. 797–828, 2012.

[3] Y. Zhu, "ADVANCED ANIONIC DOPANTS FOR POLYPYRROLE BASED ELECTROCHEMICAL SUPERCAPACITORS," 2014.

[4] J. Miller, "A brief history of supercapacitors," *Battery Energy Storage Technol.*, p. 61, 2007.

[5] P. F. Ribeiro, B. K. Johnson, M. L. Crow, A. Arsoy, and Y. Liu, "Energy storage systems for advanced power applications," *Proc. IEEE*, vol. 89, no. 12, pp. 1744–1756, 2001.

[6] B. E. Conway, *Electrochemical supercapacitors: scientific fundamentals and technological applications*. Springer Science & Business Media, 2013.

[7] B. Chu *et al.*, "A dielectric polymer with high electric energy density and fast discharge speed," *Science*, vol. 313, no. 5785, pp. 334–336, 2006.

[8] M. Armand and J.-M. Tarascon, "Building better batteries," *Nature*, vol. 451, no. 7179, pp. 652–657, 2008.

[9] R. Burt, G. Birkett, and X. Zhao, "A review of molecular modelling of electric double layer capacitors," *Phys. Chem. Chem. Phys.*, vol. 16, no. 14, pp. 6519–6538, 2014.

[10] D. V. Ragone, "Review of battery systems for electrically powered vehicles," SAE Technical Paper, 0148–7191, 1968.

[11] H. Ibrahim, A. Ilinca, and J. Perron, "Energy storage systems—characteristics and comparisons," *Renew. Sustain. Energy Rev.*, vol. 12, no. 5, pp. 1221–1250, 2008.

[12] M. Winter and R. J. Brodd, "What are batteries, fuel cells, and supercapacitors?," 2004.

[13] A. Schneuwly and R. Gallay, "Properties and applications of supercapacitors: From the state-of-the-art to future trends," *Rossens Switz.*, 2000.

[14] I. Galkin, A. Stepanov, and J. Laugis, "Outlook of usage of supercapacitors in uninterruptible power supplies," presented at the Electronics Conference, 2006 International Baltic, 2006, pp. 1–4.

[15] S. M. Rezvanizaniani, Z. Liu, Y. Chen, and J. Lee, "Review and recent advances in battery health monitoring and prognostics technologies for electric vehicle (EV) safety and mobility," *J. Power Sources*, vol. 256, pp. 110–124, 2014.

[16] B. Parkhideh, S. Bhattacharya, J. Mazumdar, and W. Koellner, "Modeling and control of large shovel converter systems integrated with supercapacitor," presented at

the Industry Applications Society Annual Meeting, 2008. IAS'08. IEEE, 2008, pp. 1–7.

[17] G. G. Amatucci, A. DuPasquier, and J.-M. Tarascon, "Supercapacitor structure," Jan. 2001.

[18] X. Xia *et al.*, "Porous hydroxide nanosheets on preformed nanowires by electrodeposition: branched nanoarrays for electrochemical energy storage," *Chem. Mater.*, vol. 24, no. 19, pp. 3793–3799, 2012.

[19] G. A. Snook, P. Kao, and A. S. Best, "Conducting-polymer-based supercapacitor devices and electrodes," *J. Power Sources*, vol. 196, no. 1, pp. 1–12, 2011.

[20] P. Sharma and T. Bhatti, "A review on electrochemical double-layer capacitors," *Energy Convers. Manag.*, vol. 51, no. 12, pp. 2901–2912, 2010.

[21] D. C. Grahame, "The electrical double layer and the theory of electrocapillarity.," *Chem. Rev.*, vol. 41, no. 3, pp. 441–501, 1947.

[22] J.-G. Wang, F. Kang, and B. Wei, "Engineering of MnO 2-based nanocomposites for high-performance supercapacitors," *Prog. Mater. Sci.*, vol. 74, pp. 51–124, 2015.

[23] A. Pandolfo and A. Hollenkamp, "Carbon properties and their role in supercapacitors," *J. Power Sources*, vol. 157, no. 1, pp. 11–27, 2006.

[24] B. Conway and W. Pell, "Double-layer and pseudocapacitance types of electrochemical capacitors and their applications to the development of hybrid devices," *J. Solid State Electrochem.*, vol. 7, no. 9, pp. 637–644, 2003.

[25] V. Augustyn, P. Simon, and B. Dunn, "Pseudocapacitive oxide materials for high-rate electrochemical energy storage," *Energy Environ. Sci.*, vol. 7, no. 5, pp. 1597–1614, 2014.

[26] H. Gao, F. Xiao, C. B. Ching, and H. Duan, "Flexible all-solid-state asymmetric supercapacitors based on free-standing carbon nanotube/graphene and Mn3O4 nanoparticle/graphene paper electrodes," *ACS Appl. Mater. Interfaces*, vol. 4, no. 12, pp. 7020–7026, 2012.

[27] M. A. Guerrero, E. Romero, F. Barrero, M. I. Milanés, and E. González, "Supercapacitors: alternative energy storage systems," *Przegląd Elektrotechniczny*, vol. 85, no. 10, pp. 188–195, 2009.

[28] P. Simon and Y. Gogotsi, "Materials for electrochemical capacitors," *Nat. Mater.*, vol. 7, no. 11, pp. 845–854, 2008.

[29] Y. Zhang *et al.*, "Progress of electrochemical capacitor electrode materials: A review," *Int. J. Hydrog. Energy*, vol. 34, no. 11, pp. 4889–4899, 2009.

[30] J. Garche, C. K. Dyer, P. T. Moseley, Z. Ogumi, D. A. Rand, and B. Scrosati, *Encyclopedia of electrochemical power sources*. Newnes, 2013.

[31] L. Vaisman, H. D. Wagner, and G. Marom, "The role of surfactants in dispersion of carbon nanotubes," *Adv. Colloid Interface Sci.*, vol. 128, pp. 37–46, 2006.

[32] P. Simon and A. Burke, "Nanostructured carbons: double-layer capacitance and more," *Electrochem. Soc. Interface*, vol. 17, no. 1, p. 38, 2008.

[33] C.-C. Hu and C.-C. Wang, "Improving the utilization of ruthenium oxide within thick carbon–ruthenium oxide composites by annealing and anodizing for

electrochemical supercapacitors," *Electrochem. Commun.*, vol. 4, no. 7, pp. 554–559, 2002.

[34] W. Kim *et al.*, "Preparation of ordered mesoporous carbon nanopipes with controlled nitrogen species for application in electrical double-layer capacitors," *J. Power Sources*, vol. 195, no. 7, pp. 2125–2129, 2010.

[35] S. Zhang and G. Z. Chen, "Manganese oxide based materials for supercapacitors," *Energy Mater.*, vol. 3, no. 3, pp. 186–200, 2008.

[36] R. N. Reddy and R. G. Reddy, "Sol–gel MnO 2 as an electrode material for electrochemical capacitors," *J. Power Sources*, vol. 124, no. 1, pp. 330–337, 2003.

[37] C. Y. Lee, H. M. Tsai, H. J. Chuang, S. Y. Li, P. Lin, and T. Y. Tseng, "Characteristics and electrochemical performance of supercapacitors with manganese oxide-carbon nanotube nanocomposite electrodes," *J. Electrochem. Soc.*, vol. 152, no. 4, pp. A716–A720, 2005.

[38] R. McNeill, R. Siudak, J. Wardlaw, and D. Weiss, "Electronic conduction in polymers. I. The chemical structure of polypyrrole," *Aust. J. Chem.*, vol. 16, no. 6, pp. 1056–1075, 1963.

[39] K. Lota, V. Khomenko, and E. Frackowiak, "Capacitance properties of poly (3, 4-ethylenedioxythiophene)/carbon nanotubes composites," *J. Phys. Chem. Solids*, vol. 65, no. 2, pp. 295–301, 2004.

[40] R. Ramya, R. Sivasubramanian, and M. Sangaranarayanan, "Conducting polymers-based electrochemical supercapacitors—progress and prospects," *Electrochimica Acta*, vol. 101, pp. 109–129, 2013.

[41] H. Lee, H. Kim, M. S. Cho, J. Choi, and Y. Lee, "Fabrication of polypyrrole (PPy)/carbon nanotube (CNT) composite electrode on ceramic fabric for supercapacitor applications," *Electrochimica Acta*, vol. 56, no. 22, pp. 7460–7466, 2011.

[42] H. Xia, M. Lai, and L. Lu, "Nanoflaky MnO 2/carbon nanotube nanocomposites as anode materials for lithium-ion batteries," *J. Mater. Chem.*, vol. 20, no. 33, pp. 6896–6902, 2010.

[43] H. Xia, Y. Wang, J. Lin, and L. Lu, "Hydrothermal synthesis of MnO 2/CNT nanocomposite with a CNT core/porous MnO 2 sheath hierarchy architecture for supercapacitors," *Nanoscale Res. Lett.*, vol. 7, no. 1, p. 33, 2012.

[44] M. Zhi, C. Xiang, J. Li, M. Li, and N. Wu, "Nanostructured carbon–metal oxide composite electrodes for supercapacitors: a review," *Nanoscale*, vol. 5, no. 1, pp. 72–88, 2013.

[45] C. Meng, C. Liu, L. Chen, C. Hu, and S. Fan, "Highly flexible and all-solid-state paperlike polymer supercapacitors," *Nano Lett.*, vol. 10, no. 10, pp. 4025–4031, 2010.

[46] D. P. Dubal, S. H. Lee, J. G. Kim, W. B. Kim, and C. D. Lokhande, "Porous polypyrrole clusters prepared by electropolymerization for a high performance supercapacitor," *J. Mater. Chem.*, vol. 22, no. 7, pp. 3044–3052, 2012.

[47] J.-H. Kim, A. K. Sharma, and Y.-S. Lee, "Synthesis of polypyrrole and carbon nano-fiber composite for the electrode of electrochemical capacitors," *Mater. Lett.*, vol.

60, no. 13, pp. 1697–1701, 2006.

[48] Y. Hu, Y. Zhao, Y. Li, H. Li, H. Shao, and L. Qu, "Defective super-long carbon nanotubes and polypyrrole composite for high-performance supercapacitor electrodes," *Electrochimica Acta*, vol. 66, pp. 279–286, 2012.

[49] K. Shi, M. Ren, and I. Zhitomirsky, "Activated carbon-coated carbon nanotubes for energy storage in supercapacitors and capacitive water purification," *ACS Sustain. Chem. Eng.*, vol. 2, no. 5, pp. 1289–1298, 2014.

[50] Y. Nogami *et al.*, "Low-temperature electrical conductivity of highly conducting polyacetylene in a magnetic field," *Phys. Rev. B*, vol. 43, no. 14, p. 11829, 1991.

[51] S. Sadki, P. Schottland, N. Brodie, and G. Sabouraud, "The mechanisms of pyrrole electropolymerization," *Chem. Soc. Rev.*, vol. 29, no. 5, pp. 283–293, 2000.

[52] S. Rapi, V. Bocchi, and G. Gardini, "Conducting polypyrrole by chemical synthesis in water," *Synth. Met.*, vol. 24, no. 3, pp. 217–221, 1988.

[53] Y. Kudoh, "Properties of polypyrrole prepared by chemical polymerization using aqueous solution containing Fe 2 (SO 4) 3 and anionic surfactant," *Synth. Met.*, vol. 79, no. 1, pp. 17–22, 1996.

[54] C. Zhou, S. Kumar, C. D. Doyle, and J. M. Tour, "Functionalized single wall carbon nanotubes treated with pyrrole for electrochemical supercapacitor membranes," *Chem. Mater.*, vol. 17, no. 8, pp. 1997–2002, 2005.

[55] Z. Zhou, N. Cai, and Y. Zhou, "Capacitive of characteristics of manganese oxides and polyaniline composite thin film deposited on porous carbon," *Mater. Chem. Phys.*, vol. 94, no. 2, pp. 371–375, 2005.

[56] V. Khomenko, E. Frackowiak, and F. Beguin, "Determination of the specific capacitance of conducting polymer/nanotubes composite electrodes using different cell configurations," *Electrochimica Acta*, vol. 50, no. 12, pp. 2499–2506, 2005.

[57] Y. S. Lim *et al.*, "Potentiostatically deposited polypyrrole/graphene decorated nano-manganese oxide ternary film for supercapacitors," *Ceram. Int.*, vol. 40, no. 3, pp. 3855–3864, 2014.

[58] J. I. Martins, L. Diblikova, M. Bazzaoui, and M. Nunes, "Polypyrrole coating doped with dihydrogenophosphate ion to protect aluminium against corrosion in sodium chloride medium," *J. Braz. Chem. Soc.*, vol. 23, no. 3, pp. 377–384, 2012.

[59] A. G. Porras-Gutiérrez, B. A. Frontana-Uribe, S. Gutiérrez-Granados, S. Griveau, and F. Bedioui, "In situ characterization by cyclic voltammetry and conductance of composites based on polypyrrole, multi-walled carbon nanotubes and cobalt phthalocyanine," *Electrochimica Acta*, vol. 89, pp. 840–847, 2013.

[60] R. Sharma, A. Rastogi, and S. Desu, "Pulse polymerized polypyrrole electrodes for high energy density electrochemical supercapacitor," *Electrochem. Commun.*, vol. 10, no. 2, pp. 268–272, 2008.

[61] H. Karamil and A. R. Nezhad, "Investigation of pulse-electropolymerization of conductive polypyrrole nanostructures," *Int. J. Electrochem Sci J*, vol. 8, pp. 8905–8921, 2013.

[62] J. Zhang, L.-B. Kong, H. Li, Y.-C. Luo, and L. Kang, "Synthesis of polypyrrole film by pulse galvanostatic method and its application as supercapacitor electrode materials," *J. Mater. Sci.*, vol. 45, no. 7, pp. 1947–1954, 2010.

[63] K. West, T. Jacobsen, B. Zachau-Christiansen, M. Careem, and S. Skaarup, "Electrochemical synthesis of polypyrrole: influence of current density on structure," *Synth. Met.*, vol. 55, no. 2–3, pp. 1412–1417, 1993.

[64] Y. Fang *et al.*, "Self-supported supercapacitor membranes: Polypyrrole-coated carbon nanotube networks enabled by pulsed electrodeposition," *J. Power Sources*, vol. 195, no. 2, pp. 674–679, 2010.

[65] S. Wencheng and J. O. Iroh, "Electrodeposition mechanism of polypyrrole coatings on steel substrates from aqueous oxalate solutions," *Electrochimica Acta*, vol. 46, no. 1, pp. 1–8, 2000.

[66] S. CHEN, "POLYPYRROLE AND COMPOSITE MATERIALS FOR ELECTROCHEMICAL CAPACITORS," 2015.

[67] Y. Zhu and I. Zhitomirsky, "Influence of dopant structure and charge on supercapacitive behavior of polypyrrole electrodes with high mass loading," *Synth. Met.*, vol. 185, pp. 126–132, 2013.

[68] P.-C. Ma, N. A. Siddiqui, G. Marom, and J.-K. Kim, "Dispersion and functionalization of carbon nanotubes for polymer-based nanocomposites: a review," *Compos. Part Appl. Sci. Manuf.*, vol. 41, no. 10, pp. 1345–1367, 2010.

[69] K. Shi and I. Zhitomirsky, "Fabrication of Polypyrrole-Coated Carbon Nanotubes Using Oxidant–Surfactant Nanocrystals for Supercapacitor Electrodes with High Mass Loading and Enhanced Performance," *ACS Appl. Mater. Interfaces*, vol. 5, no. 24, pp. 13161–13170, 2013.

[70] X. Pang, T. Casagrande, and I. Zhitomirsky, "Electrophoretic deposition of hydroxyapatite–CaSiO 3–chitosan composite coatings," *J. Colloid Interface Sci.*, vol. 330, no. 2, pp. 323–329, 2009.

[71] M. Ata and I. Zhitomirsky, "Electrochemical Deposition of Composites Using Deoxycholic Acid Dispersant," *Mater. Manuf. Process.*, vol. 31, no. 1, pp. 67–73, 2016.

[72] Y. Su and I. Zhitomirsky, "Electrophoretic nanotechnology of composite electrodes for electrochemical supercapacitors," *J. Phys. Chem. B*, vol. 117, no. 6, pp. 1563–1570, 2012.

[73] Y. Su and I. Zhitomirsky, "Electrophoretic deposition of graphene, carbon nanotubes and composite films using methyl violet dye as a dispersing agent," *Colloids Surf. Physicochem. Eng. Asp.*, vol. 436, pp. 97–103, 2013.

[74] C. Guan *et al.*, "Hybrid structure of cobalt monoxide nanowire@ nickel hydroxidenitrate nanoflake aligned on nickel foam for high-rate supercapacitor," *Energy Environ. Sci.*, vol. 4, no. 11, pp. 4496–4499, 2011.

[75] C.-W. Huang and H. Teng, "Influence of carbon nanotube grafting on the impedance behavior of activated carbon capacitors," *J. Electrochem. Soc.*, vol. 155, no. 10, pp. A739–A744, 2008.

[76] K. Shi and I. Zhitomirsky, "Electrophoretic nanotechnology of graphene–carbon nanotube and graphene–polypyrrole nanofiber composites for electrochemical supercapacitors," *J. Colloid Interface Sci.*, vol. 407, pp. 474–481, 2013.